Design and Fabrication of Electrochemical Gas Sensor

By

Muzamil Ahmad Khan

School of Chemical and Materials Engineering (SCME)

National University of Sciences and Technology (NUST)

2018

Design and Fabrication of Electrochemical Gas Sensor

Name: Muzamil Ahmad Khan

Registration No: NUST201463892MSCME67914F

This thesis is submitted as a partial fulfillment of the requirements for the degree of

MS Nanoscience and Engineering

Supervisor Name: Dr. Zakir Hussain

School of Chemical and Materials Engineering (SCME)

National University of Sciences and Technology (NUST), H-12

Islamabad, Pakistan

April 2018

Dedicated

To

All Those People

Who Inspire Me to Pursue

All of My Dreams

Acknowledgements

"Truly my prayer and my service of sacrifice, my life and my death, are (all) for ALLAH, the Rabb (Only God, Cherisher and Sustainer) of the Worlds". (Quran 6:162)

First and foremost, I would like to express my sincere gratitude to my supervisor, **Dr. Zakir Hussain** for all his tremendous support, and encouragement. Without his continuous optimism, enthusiasm and patience this thesis would not have been possible. His guidance into the world of sensors and electrochemistry has been vital during my post graduate studies. I will always be grateful for an opportunity to work in his research group and to learn from him.

I would like to thank my committee members, **Dr. Iftikhar Hussain Gul** and **Dr. Ahmad Nawaz Khan** for their participation in my thesis committee.

I greatly acknowledge the guidance of **Dr. Aftab**, for providing advice and expertise in cyclic voltammetry technique.

I am also grateful to the whole staff of School of Chemical and Materials Engineering NUST for their extreme co-operation and friendly behavior.

I am truly thankful to my best friends especially **Mr. Umair Idrees, Mr. Zohaib Kamal, and Mr. Amaar Ahmed** for their emotional support and continuous encouragement.

Finally and most importantly, I would like to express my deepest gratitude to my most loving **Grandmother** who always kept praying for my success (and I'm sure that she still keeps doing that from the heavens) and my whole **family** especially **parents**. My family has made my post-graduate studies possible; even from a distance they kept supporting me and my words cannot express how grateful I am for their immense love and support. I thank them for believing in me.

Muzamil Ahmad Khan

Abstract

This thesis manifests the fabrication of electrochemical gas sensor by chemically modifying copper based interdigitated electrodes (IDEs) with various nanomaterials. Five electrochemical sensors for ammonia (NH_3) gas sensing and five electrochemical sensors for carbon dioxide (CO_2) gas sensing have been prepared.

A simple, fast and low-cost method of fabricating copper based interdigitated electrodes (IDEs) is presented. The fabrication process employed, involves fewer processing steps and cheap materials. Layout of the circular interdigitated electrode with diameter of 17.5mm is designed using CAD software and scanned onto a transparent film to make a positive mask of it. This positive mask is used to impose the design on a screen used in screen printing technique and the design is transferred onto the copper clad board by using PVC black printing ink. The ink acts as an etch resist in a ferric chloride solution. The layout design of the obtained IDE is observed under an optical microscope and is found same as in the CAD layout.

Co-precipitation route has been employed for the successful synthesis of nickel magnesium ferrite ($Ni_{0.5}Mg_{0.5}Fe_2O_4$) and it's composite with reduced graphene oxide (rGO) has been obtained through physical method by ultrasonication technique.

Electrochemical gas sensors for investigating the electrochemical response towards various concentrations of NH_3 and CO_2 gases were developed by the modification of IDEs with $Ni_{0.5}Mg_{0.5}Fe_2O_4$ nanoparticles, graphene oxide (GO), rGO and $Ni_{0.5}Mg_{0.5}Fe_2O_4$/rGO nanocomposite. The modifiers (sensing materials) were characterized by using powder X-ray diffraction (XRD) and scanning electron microscopy (SEM) for their structural and morphological studies. The SEM results of $Ni_{0.5}Mg_{0.5}Fe_2O_4$ nanoparticles confirmed the spherical morphology of nanoparticles with the average particle size to be 20nm without any agglomeration and SEM micrograph of nanocomposite showed that these spherical nanoparticles are homogenously distributed on graphene sheets. The XRD results showed that all the relevant peaks are present, thus justifying the formation of required sensing materials.

. The electrochemical response of the chemically modified IDEs exposed to different concentrations of NH_3 and CO_2 gases in 0.1M NaOH electrolyte has been established through cyclic voltammetry. The cyclic voltammograms obtained reveal that all the modified IDEs show considerable change in current before and after exposure to the gases (analyte). The maximum response towards various gas concentrations of NH_3 and CO_2 was shown by the $Ni_{0.5}Mg_{0.5}Fe_2O_4$/rGO nanocomposite modified IDE while as bare electrode showed very limited change in the response followed by $Ni_{0.5}Mg_{0.5}Fe_2O_4$ nanoparticles modified IDE. The sensitivity and limit of detection (LOD) of $Ni_{0.5}Mg_{0.5}Fe_2O_4$/rGO nanocomposite modified IDE towards various concentrations of NH_3 gas have been calculated. The sensitivity achieved by using $Ni_{0.5}Mg_{0.5}Fe_2O_4$/rGO nanocomposite as a sensing element was found to be 0.000713023 A ppm^{-1} and limit of detection (LOD) obtained was 17.1 ppm, which is below the threshold limit of 25ppm set by the world health organization (WHO).

Table of Contents

List of Figures

List of Tables

List of Abbreviations:

SEM	Scanning Electron Microscope
XRD	X-Ray Diffraction
CV	Cyclic Voltammetry
IDE	Interdigitated Electrode
NMF	Nickel Magnesium Ferrite
GO	Graphene Oxide
rGO	Reduced Graphene Oxide
CAD	Computer Aided Design
PVC	Poly Vinyl Chloride
CME	Chemically Modified Electrode
SCE	Saturated Calomel Electrode

Chapter 1

Introduction

A sensor is a device that detects a particular analyte or substance and transmits it as a signal to a measuring or control instrument. Sensors are mainly designed to detect and respond to an analyte in the solid, liquid or the gaseous state [1]. On the basis of response to be detected, sensors are broadly classified as physical sensors and chemical sensors. Physical sensors detect physical responses such as mass, temperature, strain, pressure etc., while as; chemical sensors have a chemical reaction or molecular analyte to be measured [2].

1.1 Chemical Sensor

A chemical sensor can be defined as a device that transforms any chemical information such as, composition, ionic change, and change in concentration or any other chemical activity, etc., into an analytically useful signal. This chemical information originates from a chemical reaction of the analyte or from a physical property of the system under investigation. All chemical sensors consist of a chemically selective layer and a transducer. The transducer transforms the chemical (analytical) information into a detectable signal by means of electrical instrumentation and the chemically selective layer isolates the response of the analyte from its immediate environment. Chemical sensors are of many types and depending on the transducer type can be classified as: thermal [3], optical [4], mass [5] or electrical sensors [6]. Development in the field of analytical chemistry reveals that electrochemical sensors are the most rapidly growing class of chemical sensors. Compared to optical, mass and thermal sensors, electrochemical sensors are important due to their enhanced detectability, experimental simplicity, low cost, high sensitivity and selectivity [7].

1.2 Electrochemical Sensor

1.2.1 Brief History

History of electrochemical sensors reveals that this group of chemical sensors is the largest and the oldest group with first sensor used in 1950s for oxygen monitoring. Since mid-1980s, miniaturized electrochemical sensors that could measure a multitude of different chemical species were available at industrial levels. As of 2012, electrochemical sensors comprised of almost 58% of total chemical sensors [8, 9].

1.2.2 Applications

Electrochemical sensors have found diverse applications in various fields; such as, petrochemical industries, biological diagnostics, medicine, environmental monitoring etc., (Figure 1). One of the most important applications of electrochemical sensors is monitoring of environmental contaminants. Due to rapid industrialization, large-scale agriculture and mining; the environment in which living organisms live, work or breathe is subjected to constant contamination due to disposal of toxic contaminants from industries such as heavy metals (Cr, Pb, As, Hg) and toxic gases (NH_3, CO, SO_2, H_2S). These harmful additions to the environment cause serious complications to the human health; for example CO, if inhaled at above 35ppm concentration is very dangerous to hemoglobin, SO_2 causes strong irritation to eyes including coughing and prolonged exposure to Pb^{2+} ions even at very low concentrations can cause kidney failure, renal malfunctioning and brain damage [10, 11]. The continuous increase of these toxic contaminants in the environment demands the need of developing sophisticated yet simple and low cost detection methods. This need is must to keep the toxic levels in the environment under control and electrochemical sensors have shown a promising potential to be well suited for this need.

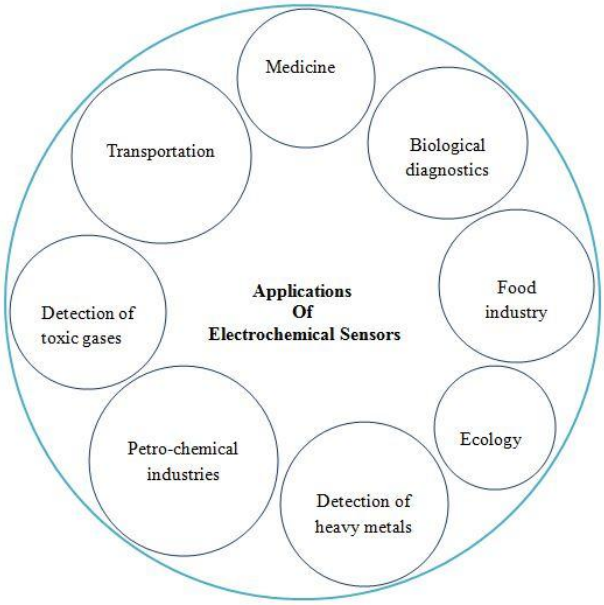

Figure 1. Applications of Electrochemical Sensors [11]

1.2.3 Definition

Electrochemical sensor is a type of chemical sensor in which the analytical information is obtained from the electrical signal (such as; current, impedance or voltage) resulting from the interaction of target analyte and the transducer covered with a chemical recognition layer [12]. Electrochemical gas sensors are gas detectors that measure the concentration of the target gas by oxidizing or reducing it at an electrode and measuring the resulting current [13].

1.2.4 Working Principle of Electrochemical Gas Sensor

Working principle of electrochemical gas sensors include an operation that is based on the diffusion of target gas into the sensor, which produces an electrical signal proportional to the gas concentration. The gas of interest first passes through a small capillary-type opening and before coming in contact with the sensing electrode surface, it has to diffuse through a porous membrane. At the surface of the sensing electrode, the diffused gas gets oxidized or reduced as a result of which, a sufficient amount of electrical signal is produced. The assembly of a typical electrochemical gas sensor (Figure 2) consists of a sealed chamber that has a small opening for target gas input, a permeable membrane through which the gas diffuses onto the sensing electrode (SE), also known as working electrode (WE) and after oxidization or reduction of gas at the sensing electrode surface, the electrons produced are collected

at the counter electrode (CE) causing the flow of a electric current. This current flow produces an appreciable electric signal that is interpreted using proper instrumentation. A third electrode known as a reference electrode (RE) is incorporated into the assembly to keep the potential of the sensing electrode at constant value that otherwise fluctuates due to constant reaction resulting in degradation of sensor performance. This reference electrode has no external current associated with it. The three electrodes involved are connected through an electrolyte [11].

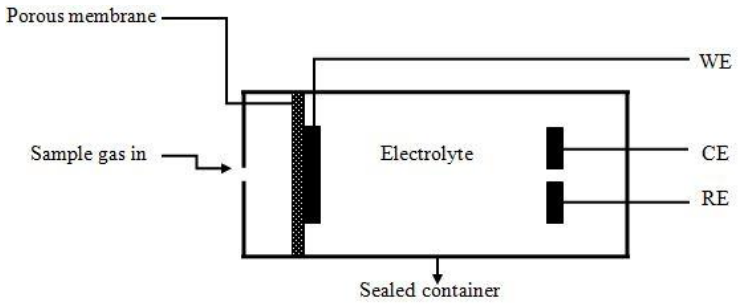

Figure 2. Schematic showing assembly of a typical electrochemical gas sensor [11].

The main emphasis of this work is to fabricate a very low cost electrochemical gas sensor that can detect gases with higher sensitivity and minimum limit of detection possible. The fabricated sensor has been successfully tested in laboratory to sense NH_3 and CO_2 gases.

1.3 Electroanalytical Methods

Electroanalytical methods encompasses a group of techniques in analytical chemistry that involve study of an analyte by measuring electrical properties such as potential (volts) and/or current (amperes) of the analyte contained in an electrochemical cell. Such techniques have the benefits of giving diverse characterization information and producing low detection limits in systems involving electrochemical processes [14-17]. Measurements through electroanalytical or electrochemical techniques offer various advantages:

(a) Specificity

(b) Selectivity – depends on the choice of electrode material

(c) Low detection limits
(d) Higher degree of sensitivity
(e) Close to real time results – in many cases real time results
(f) Miniaturized sensors – this application comes to play where other sensors fail to operate.

Electrochemical measurements have two-dimensions with potential related to qualitative properties (controlled by thermodynamics or kinetics) and the current related to quantitative properties (with control from either mass transport process or reaction rates). The principle criterion for electroanalytical measurements is that the analyte (or species under examination) should react with the electrode. The reaction of analyte with the electrode is possible in following three ways:

(a) Directly,
(b) Indirectly, through coupled reaction, and
(c) Adsorption of analyte onto the electrode.

Electrochemical measurements are possible only in situations that have sufficiently conducting medium (electrolyte) between the two electrodes comprising the electrical circuit. Depending on which aspects of the electrochemical cell are controlled and which are measured, electroanalytical methods are divided into three main categories, namely:

(a) Potentiometry,
(b) Coulometry, and
(c) Voltammetry/Amperometry.

In *potentiometry*, the potential of an electrochemical cell under static conditions is measured and no current or negligible current flows through the electrochemical cell while its whole composition remains unchanged.

Coulometry involves the measurement of the quantity of electricity (in coulombs) needed to convert the analyte quantitatively from one oxidation state to another at the working electrode. In coulometry, current is monitored as a function of time.

In *voltammetry*, a time-dependent potential to an electrochemical cell is applied and the resulting current as a function of applied potential is measured. The applied potential is varied systematically to cause oxidation or reduction of the electroactive chemical species at the working electrode. The plot of current versus applied potential is called as a voltammogram. If the operating potential is fixed (not

varied) and the resulting current is measured as a function of time; this voltammetric technique is known as *amperometry*. Since potential is fixed, amperometry does not result in a voltammogram.

In the present study, voltammetric method for electrochemical measurements of fabricated electrochemical sensor has been chosen. So, this electrochemical sensor can also be called a voltammetric sensor.

1.4 Voltammetric Sensor

It is an electrochemical sensor that operates by measuring the current response with respect to the potential applied over a varied range i.e., between initial and final values of potential (E); in simpler terms, it works by registering current – potential profiles known as voltammograms.

This type of sensor operates on a three-electrode system, which includes a *working* or *sensing electrode*, a *reference electrode* and an *auxiliary* or *counter electrode.* These three electrodes are connected to a specially designed circuit called as a *potentiostat* that is used for precise controlling of the potential applied to the working electrode. The voltammetric measurements by the potentiostat are usually performed in a solution containing excess inert salt called *supporting electrolyte*. The data acquisition of electrochemical response and control of potentiostat is performed on a computer interface attached to it through supporting software (Figure 3) [18, 19].

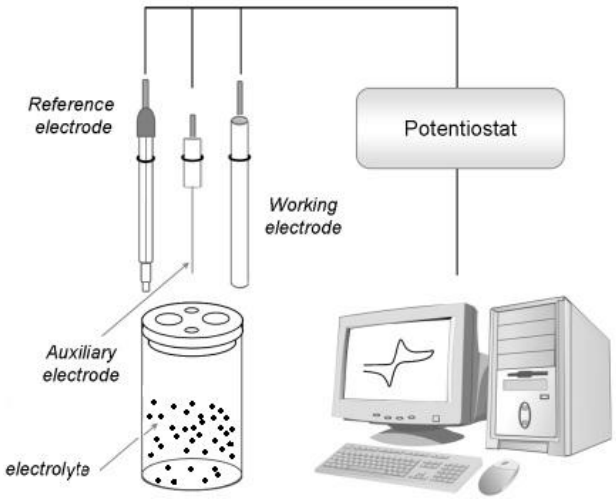

Figure 3. Typical electrochemical cell with a three electrode system [19]

1.4.1 Working Electrode

The electrode in an electrochemical system at which the reaction of interest takes place is called working electrode. This electrode usually shows a substantial change in potential when a very small current passes through, making it an ideally polarizable electrode. The working electrodes are usually made from inert materials, such as metals (Hg, Pt or Au) or allotrope derivatives of carbon (graphite or glassy carbon) [19]. To improve the performance of electrochemical sensing systems, interdigitated assembly of conducting electrodes have been widely used [20-23]. In this study, the working electrode applied for sensing purpose is a conducting interdigitated electrode modified with a sensing layer.

1.4.2 Interdigitated Electrodes

Interdigitated electrodes (IDEs), in simpler terms, can be defined as a two 'comb-shaped' electrodes in which the teeth of one comb (generator electrode) are aligned in between the teeth of another comb (collector electrode) separated by a very small gap as shown in Figure 4 [24]. Due to their geometrical differences from the conventional electrodes, IDEs result in much improved electrochemical responses. The electroactive species generated at the generator electrode are collected at the collector electrode where they get electrolyzed and are diffused back to the generator (redox cycling); this phenomenon amplifies the currents at both electrodes of IDEs [25, 26]. IDEs are used in applications that include non-destructive testing, biotechnology, telecommunications, and are widely used in electrochemical sensing applications, such as biosensor, gas sensor, humidity sensor and many more. IDEs detect the electrical signals generated by sensing materials, thus function as a main component of the electrochemical sensors. As an example of a humidity sensor, a polymer film is deposited on an interdigitated electrode which functions as a dielectric between the electrodes. This polymer film absorbs or releases moisture due to the relative ambient humidity that changes its dielectric properties (permittivity); causing change in the capacitance which gets monitored [27, 28].

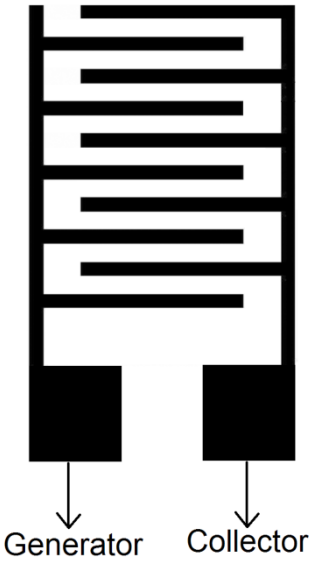

Figure 4. Schematic of a comb shaped interdigitated electrode

Materials used to fabricate the IDEs are mostly metals with excellent conductivity that include aluminium, gold, platinum, silver and copper [29, 30]. Generally, photolithography technique is used for the fabrication of microstructures including IDEs. However, photolithography process employs many steps and requires the use of sophisticated equipment. Therefore, in recent years efforts have been made to simplify the fabrication process for IDEs. For low-cost manufacturing and shorter development time, many alternative and simpler methods have been used that include inkjet printing, stamps and screen printing [28, 31].

1.4.3 Reference Electrode

A reference electrode is a non-polarizable electrode that provides a stable and fixed potential to the electrochemical cell against the potential applied to the working electrode. The reference electrode has a well known electrode potential because of which working electrode potential is measured and controlled. The most commonly used reference electrodes are silver – silver chloride ($Ag/AgCl_{(sat)}$), saturated calomel electrode (SCE), and standard hydrogen electrode (SHE) [19]. In this work, SCE was used as a reference electrode.

1.4.4 Counter Electrode

The counter electrode, also known as auxiliary electrode, is a current conducting electrode necessary for completion of circuit in an electrochemical cell. Since, reference electrode has fixed potential value; therefore, any change (redox process) in the cell is due to the other two electrodes. For an electrode to act as a counter electrode, it must satisfy certain conditions:

(a) It must not dissolve in the medium (electrolyte) of the electrochemical cell.
(b) Reaction product generated at this electrode should not react at the working electrode.
(c) Its electrode area must be larger than that of working electrode so that this area doesn't affect the limiting current.

The counter electrodes normally consists of a platinum wire and in many cases carbon electrodes. In the present work, carbon rod has been used as a counter electrode.

1.4.5 Supporting Electrolyte

All inert ionic salts or ionizable compounds in a solvent are defined as supporting electrolytes. The inertness mentioned here indicates its ability to avoid oxidation or reduction at the working electrode during electrochemical measurements. Supporting electrolytes perform three important functions as mentioned below:

(a) It carries most of the ionic current of the cell as its concentration is much higher than other species in the solution; thus keeping the cell resistance at a low value and completing the circuit of the cell.
(b) It maintains a constant ionic strength.
(c) It suppresses the effect of the migration current that arises due to movement of ions caused by an electric field produced due to potential difference between the working and counter electrodes of the electrochemical cell.

KCl is the mostly used supporting electrolyte salt because it is easily available in high purity form and the mobility of both potassium and chloride ions is almost equal. Various other supporting electrolyte salts used are KNO_3, KOH, NaOH

etc., in alkaline medium and for studies in acidic aqueous solutions H_2SO_4, HCl etc., are normally employed. In neutral regions buffer solutions such as of acetate, citrate and phosphate buffers are usually used [15].

1.4.6 Potentiostat

A potentiostat is a specially designed electronic circuit (hardware) that is employed to run most of the electroanalytical experiments and is especially used to control a three electrode electrochemical cell. A potentiostat basically helps in controlling the potential of the working electrode. If a potentiostat is able to control two working electrodes it is called a bipotentiostat; similarly, a polypotentiostat is a potentiostat capable of controlling more than two working electrodes. Various manufacturing units that deliver potentiostats equipped with latest instrumentations and technologies include Gamry, DropSens, BioLogic etc. In this study, Gamry Series G750 Potentiostat has been used to perform electrochemical measurements.

1.4.7 Chemically Modified Electrodes

Chemically modified electrode (CME) is an electrode made of a conducting or semi-conducting material that is modified by coating of a selected mono - or multi – molecular film, ionic film or polymeric chemical film and due to charge-consuming (Faradaic) reactions show chemical, electrochemical and/or optical properties of the chemical film. Compared to other electrode concepts in electrochemistry, such electrodes accomplish a broad range of functions in electrochemical devices such as in chemical sensing, energy storage, energy conversion, electronics and electrochromic displays that change color on oxidation and reduction. Most importantly, such electrodes are used in analytical sensors that are selective for particular species [32].

Various substrates (coatings) such as carbon nanotubes (CNTs) [33, 34], ferrite nanoparticles [35, 36], polymer films [37, 38], nano-composites [39, 40], reduced graphene oxide [41, 42] etc are used for the modification of various electrode surfaces such as glassy carbon, interdigitated, gold electrodes etc., Most of these modifications have been done to improve the sensing capabilities of the electrodes. For the present study, an interdigitated electrode has been modified with

ferrite nanoparticles (Ni-Mg), rGO and nanocomposite of these two for electrochemical sensing purposes.

1.5 Voltammetric Techniques

While performing voltammetry, three important experimental parameters can be controlled, that are:

(a) Changing of potential applied to the working electrode,
(b) When to measure the current, and
(c) Whether to stir the solution or not.

There are a number of voltammetric techniques that can be employed for electrochemical measurements and most commonly used are listed as follows:

(a) Polarography,
(b) Hydrodynamic voltammetry,
(c) Pulse voltammetry,
(d) Stripping voltammetry,
(e) Linear sweep voltammetry (LSV), and
(f) Cyclic voltammetry (CV).

In the present study the electrochemical measurements were performed through cyclic voltammetry technique.

1.5.1 Cyclic Voltammetry

Cyclic voltammetry (CV) is a type of voltammetric technique which is used to determine the electrode reaction mechanisms, diffusion coefficients and standard electron transfer rate constants [43]. In CV, varied potential is applied at a working electrode in both forward and reverse directions and in result current is produced that is plotted against the applied potential. For CV characterization, a typical three-electrode cell is used that includes a working electrode, an auxiliary electrode and a reference electrode (Figure 3). The potential applied to the working electrode vs. the reference electrode is controlled through the potentiostat, while compensating for as much of the cell resistance as possible [44]. To complete the electrical circuit, counter electrode is used.

In cyclic voltammetry, Faradaic current is measured as a function of the applied potential, and this current provides the information about the analyte under examination. In CV, the potential is swept in a linear manner from an initial potential value to the final or limiting potential value and the response of the current over this potential range is measured. The direction of the potential scan is reversed on final potential value and now the scanning take place over the same potential range but in the opposite direction (that is why it is called "cyclic"). As a result, oxidation generated species (on the forward scan) get reduced on the reverse scan [45]. The time taken to sweep the range is determined by the Scan rate (mV/s).

The obtained potential v/s current plot from a reversible redox couple is called a cyclic voltammogram featuring various parameters as shown in Figure 5. The important parameters obtained from a typical voltammogram are peak potentials (E), peak currents (i) and the potential difference ΔE between the oxidation (O) and reduction (R) peaks. The electron transfer mechanism of the electrode is obtained to an extent, using these parameters [46].

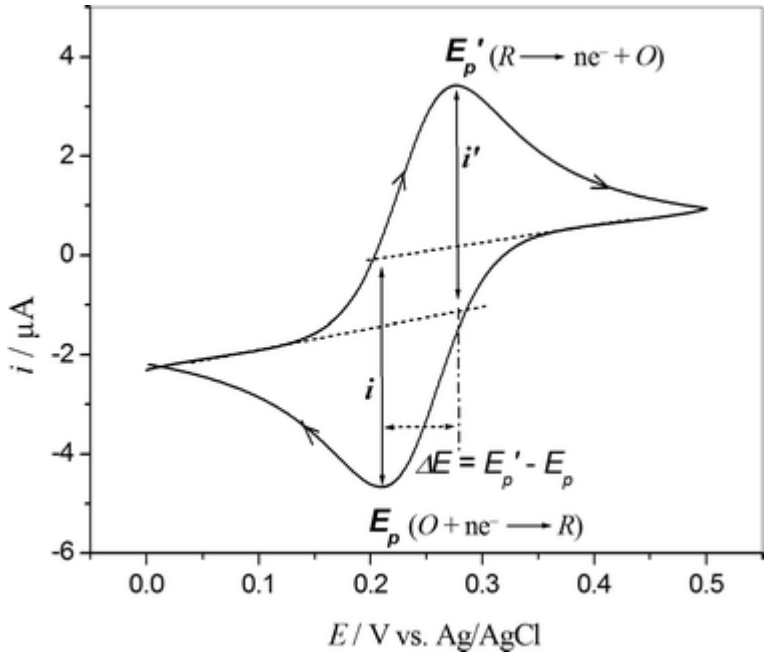

Figure 5. A typical cyclic voltammogram showing important parameters of a reverse redox couple [46].

1.6 Need for Electrochemical Detection of Ammonia

Ammonia (NH_3) is a colorless, pungent toxic gas emitted by industries and automobiles whose permissible maximum concentration is 50 ppm. It is considered dangerous if inhaled at 2500-6500 ppm for more than 2 hours. Such prolonged exposure to ammonia can develop sensory, respiratory and cardiovascular complications leading to chronic diseases or even death. Hence for the trace level detection of ammonia in medical, industrial and environmental areas; development of reliable and affordable gas sensors is very important [47, 48]. Various types of sensors for the detection of ammonia have been used that include metal oxides (catalytic), optical and electrochemical sensors. However, due to high sensitivity, low power consumption and relatively low cost; electrochemical gas sensors are widely used [49]. Over the past decade a vast research has been done on the electrochemical detection of NH_3 due to incorporation of nanomaterials [50-60].

1.6.1 Scope of the Present Work

In the present work a simple, low cost and fast method has been used to fabricate copper based interdigitated electrodes. These electrodes were chemically modified using thin films of various nanomaterials such as $Ni_{0.5}Mg_{0.5}Fe_2O_4$ ferrites, rGO, PAni polymer and their nanocomposite. These chemically modified electrodes were used as the working electrodes in the voltammetric measurements using NaOH electrolytic solution whose concentration was altered by different concentrations of NH_3 gas (analyte). Cyclic voltammetry technique has been used for electrochemical measurements and it was noticed that specific electrochemical response against different concentrations of analyte was obtained indicating its scope as a voltammetric sensor for NH_3 detection. The fabricated sensor has also been tested for CO_2 response in order have broader look at its electrochemical responses.

Chapter 2

Experimental

The experimental portion of the present work is divided into three main portions:

(a) Fabrication of interdigitated electrodes,
(b) Synthesis and characterization of sensing materials, and
(c) Fabrication of chemically modified electrodes as voltammetric sensors.

2.1 Chemicals and Materials

Acetone (AnalaR) was purchased from Fisher Scientific (BDH Laboratory Supplies). Ferric chloride ($FeCl_3$, anhydrous, powder, 99.99%) was obtained from Sigma Aldrich. Potassium hydroxide (KOH, 85%) was purchased from Riedel-de-Haen (Sigma-Aldrich) and Sodium hydroxide (NaOH, 96%) was obtained from Merck.

A binary standard solution (ethanol/water) was prepared by diluting the ethanol in ultrapure water (conductivity 0.35 S/m) that was processed through a water purification system (TKA Smart2Pure - Thermo Scientific). Copper clad board was purchased from local electronics market (cost ~ 2$).

$Ni(NO_3)_2.6H_2O$ (99.9% purity, Merck), $Mg(NO_3)_2.6H_2O$ (99.9% purity, Sigma Aldrich), $Fe(NO_3)_3.9H_2O$ (99.9% purity, Sigma Aldrich), NaOH (99.9% purity, Sigma Aldrich), Graphene Oxide (Graphene market, USA), Hydrazine hydrate were used All materials used were of analytical grade and used without further treatments.

For polyaniline synthesis, aniline monomer $C_6H_5NH_2$ (Sigma-Aldrich, >99.9%), HCl (Sigma-Aldrich, >99.9%) and ammonium persulfate $(NH_4)_2S_2O_8$ (Sigma-Aldrich, >99.9%) were used.

2.2 Fabrication of Interdigitated Electrodes (IDEs)

Copper based IDEs were fabricated by using a single sided copper clad board (used for printed circuit boards in electronics) having dimensions 300mm x 150mm x 1.5mm. This board consisted of 0.035mm thick layer of copper laminated on FR4 composite material (glass-reinforced epoxy laminate material). Since copper layer easily gathers oxide layer, super fine sand paper with 600 grit size was used to remove this layer by slightly scrubbing the surface under running water. The obtained bright metallic copper surface was purified by washing with ultrapure water and ethanol. After complete drying, this board was kept in an air tight chamber so that further oxidation on the surface can be prevented.

The IDE template was created using Autodesk Autocad 2015 software. Total diameter of the circular IDE was 17.5mm with each electrode finger having 0.35mm thickness and interdigital space of 1.25mm. The designed IDE had a total of 6 fingers and 2 contact pads (3mm x 4mm). The CAD design of IDE is given in Figure 6.

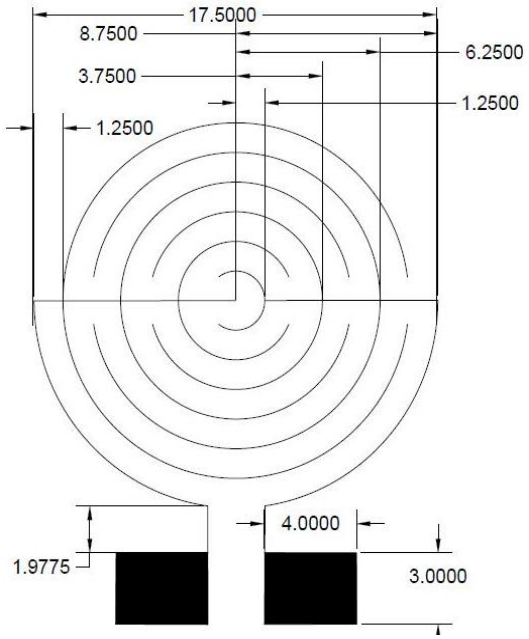

Figure 6. CAD design and dimensions of circular IDE

To generate the mask, the CAD design was transferred onto a transparent film by scanning. The scanning method involves the concept of computer to screen (CTS) imaging system and by using the generated mask, the digitized image of IDEs was

reproduced onto the copper board by screen printing process. The PVC printing ink was used to reproduce the designed image of IDE on the cleaned surface of copper board. After the ink completely dried on its own, any exposed copper that was not masked by the PVC ink was etched out via exposure to $FeCl_3$ solution (42% w/v in ultrapure water) in Pyrex tray placed in closed fume hood. The whole etching process took 15 to 20 minutes to complete. The etched board was then sprayed with acetone and cleaned with cotton swabs, so that the PVC ink gets removed from the copper board, exposing the designed IDEs. Figure 7 shows the pictorial representation of IDE fabrication.

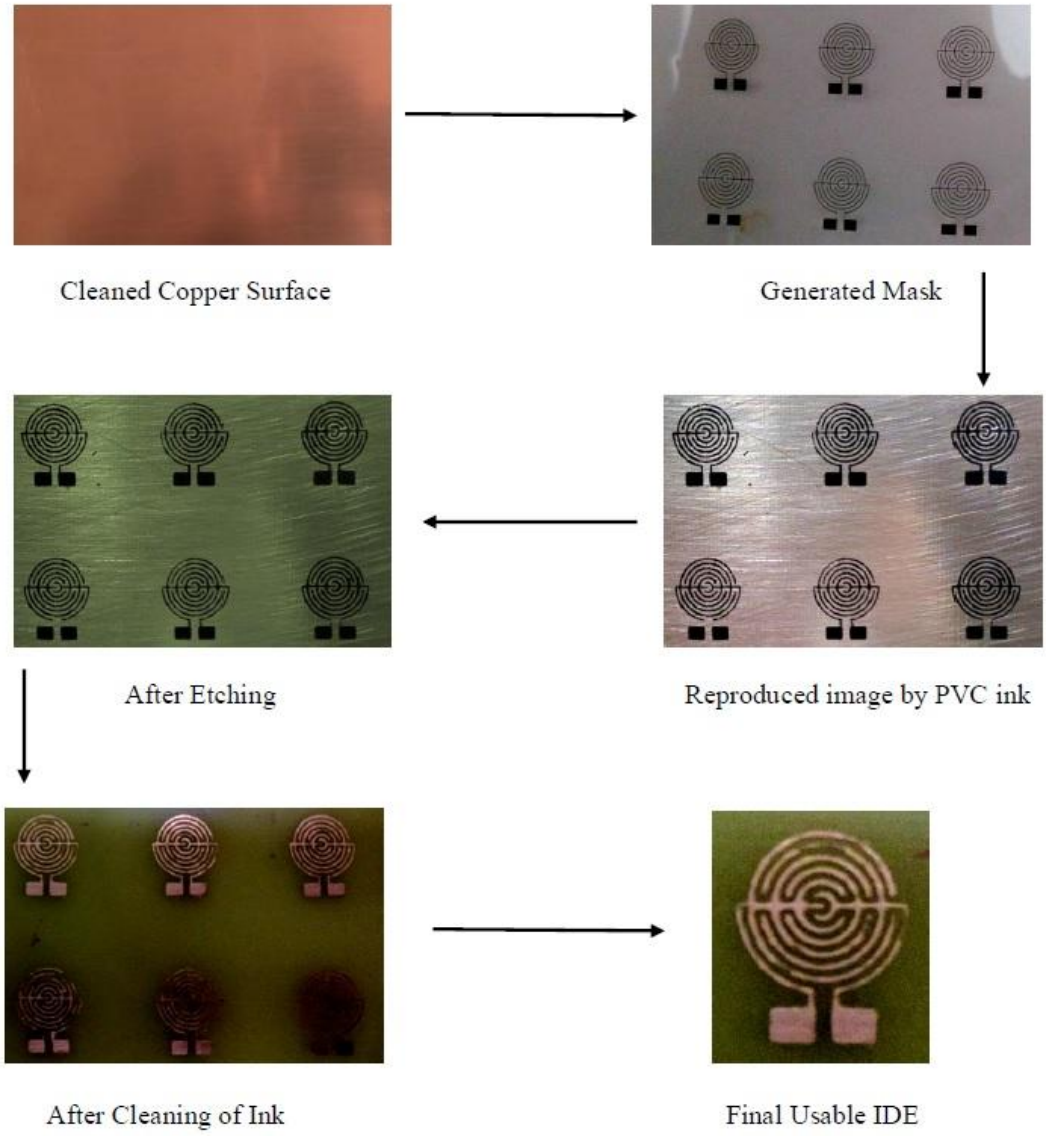

Figure 7. Pictorial representation of IDEs Fabrication

Low speed precise SAW (MODEL DTQ 5) was used to finely cut the board and separate all the fabricated IDEs, so that individual interdigitated electrode could be obtained for electrochemical analysis. Every obtained IDE was tested by using a UT60A (UNI-T) digital multimeter (DMM) to check the connectivity and any IDE found short circuited was discarded. The remaining IDEs were further analyzed under Optika light microscope at 5X magnification to sort out the complete printed IDEs and any half printed or disconnected finger based IDEs were rejected also. Only, IDEs resembling to original CAD design dimensions were kept for electrochemical applications.

The obtained IDEs were further cleaned through the same procedure as mentioned above by using 600 grit super fine sand paper, ultrapure water and ethanol. The final thickness of copper layer measured by digital Vernier Caliper was 0.025±0.002mm, rest being removed through the cleaning process. The thickness of copper layer was measured by subtracting the thickness of etched part of board (without copper layer) from thickness of un-etched part of board (with copper layer). Finally, all the usable IDEs were stored in an air tight chamber to prevent oxidation or any sort of impurity that may stick to them.

2.3 Synthesis of Sensing Materials

2.3.1 Synthesis of $Ni_{0.5}Mg_{0.5}Fe_2O_4$ Ferrites (NMFs)

The NMF nanoparticles were synthesized through the co-precipitation route [61] with stoichiometric ratio taken as 0.5:0.5:2. The amounts of initial precursors taken for the preparation of NMF nanoparticles are given as:

i. 18.90 mg of hydrated nickel nitrate [$Ni(NO_3)_2.6H_2O$] salt,
ii. 16.67 mg of hydrated magnesium nitrate [$Mg(NO_3)_2.6H_2O$] salt, and
iii. 525.2 mg of hydrated iron nitrate [$Mg(NO_3)_3.9H_2O$] salt.

Three beakers containing 100ml ultrapure water with magnetic stirrer each were taken and the initial precursors were added to these separate beakers. Each beaker was placed on the hot plate for almost 15 minutes in order to form dispersions of the salts through continuous stirring. A 500ml beaker was taken and the obtained dispersions were mixed in it. By putting a magnetic stirrer in it, this beaker was placed on a hot plate for continuous stirring and 3M sodium hydroxide (NaOH) was

added drop by drop to neutralize this solution. This overall reaction took place for almost 45 minutes and was carried out at 85^{o}C. Once the reaction was complete, the stirring was stopped and the obtained solution was kept as such for overnight so that the precipitates formed could settle down. After settling of the precipitates, excess water from the beaker was discarded and the precipitates were collected. The obtained precipitates were washed with distilled water several times so that pH value of 7 could be obtained and the water gets free of all the sodium and nitrate ions. Once the washing process was complete, the obtained product was kept in an oven at 110^{o}C for one night to completely dry it. After complete cooling, the product was taken out and by mortar and pestle this product was grinded to obtain a fine powder. This powder was sintered at 600^{o}C for withholding time of 4 hours and after sintering was complete fine NMFs nanoparticles were obtained [61-63]. Figure 8 shows the pictorial representation of the NMFs synthesis.

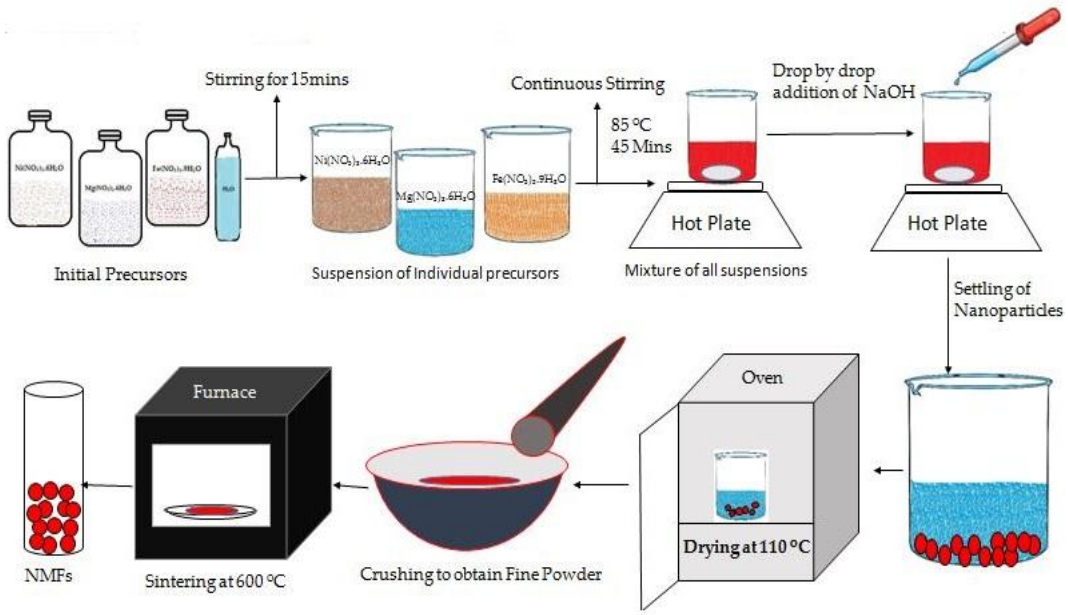

Figure 8. Pictorial representation of NMFs synthesis

2.3.2 Synthesis of $Ni_{0.5}Mg_{0.5}Fe_2O_4$ /rGO nanocomposite (NMF-rGO)

Ultra-sonication method was used to synthesize the nanocomposite of NMFs and reduced graphene oxide (rGO) [64]. A graduated beaker containing 5ml of ultrapure water was taken and 2mg of GO was added to it. This beaker was later put in a sonication bath for 30 minutes of sonication time. After first stage of sonication,

5mg NMFs were added to this solution and further sonication was performed for 30 more minutes so that both GO and NMFs are physically mixed. Once the second stage of sonication is completed, 1ml of hydrazine hydrate was added to this solution and again sonication was performed for 60 minutes. Hydrazine hydrate was added for reduction of GO to rGO. After all the sonication process was done, the solution was taken out of the sonication bath and centrifuge washing (3 times at 4000 rpm for 30 minutes at room temperature) by using distilled water to this solution was performed. The product obtained was dried in an oven at 80^{o}C. The dried product was annealed in N_2 atmosphere at 250^{o}C for 60 minutes at the heating rate of 10^{o}C min^{-1} [64, 65]. Figure 9 shows the pictorial representation of the NMF-rGO synthesis.

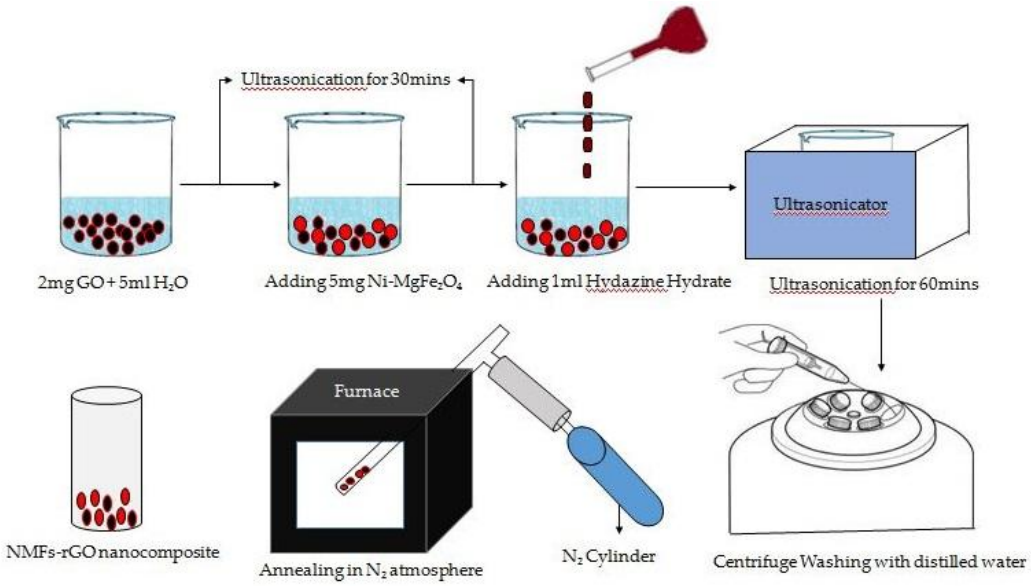

Figure 9. Pictorial representation of NMF-rGO synthesis

2.3.3 Dispersions of the Sensing Materials

2% w/w dispersions of 4 sensing materials viz., NMFs, GO, rGO, and NMF-rGO nanocomposite in de-ionized water were prepared. For 2% w/w composition, four 2ml viols were taken and each viol was filled with 0.392ml de-ionized water. Now, 8mg from each sensing material i.e., NMF, GO, rGO and NMF-rGO was dispersed in each of the viol respectively. The viols were sonicated for 90 minutes so that clear dispersions of sensing materials in de-ionized water could be achieved.

2.4 Fabrication of Chemically Modified Electrodes as Voltammetric Sensors

A total of 4 IDEs were taken and each was chemically modified by 1 type of sensing material (NMFs, GO, rGO and NMF-rGO); so that 4 different chemically modified IDEs are obtained. This chemical modification was achieved by drop casting 20μL amount from each of the sensing material dispersions on IDEs. These modified electrodes were left to dry at room temperature for 2 hours. After complete drying, a very thin layer of sensing material was casted on IDEs. It is these film deposited IDEs that act as voltammetric sensors and their sensing capabilities were recorded by using them as working electrodes in the three electrode system of potentiostat. Figure 10 shows the pictorial representation of film deposited circular IDEs.

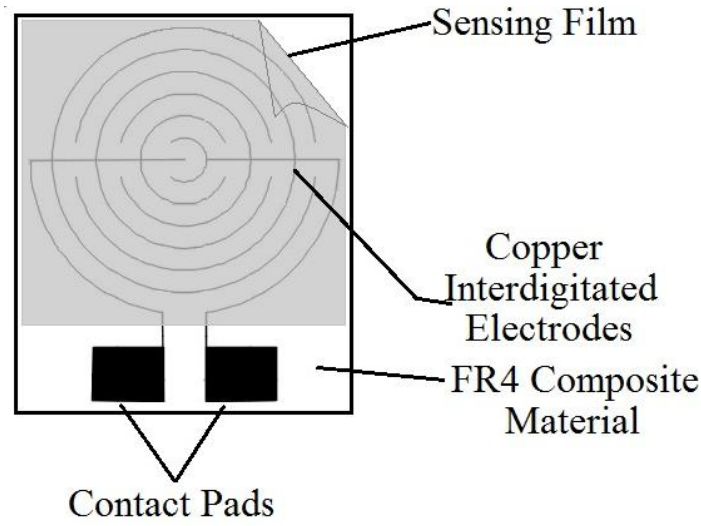

Figure 10. Top view of the chemically modified IDE (voltammetric sensor)

2.5 Setup for Electrochemical Characterization of Voltammetric Sensors

The electrochemical response (sensing capabilities) of the voltammetric sensors were performed through cyclic voltammetry (CV) by using Gamry made potentiostat (G750) that incorporates three electrode system. The chemically modified IDE (voltammetric sensor) acted as a *working electrode*, saturated calomel electrode (SCE) fitted in a reference electrode bridge tube was used as a *reference electrode* (shown in Figure 12a and 12b), and graphite rod (0.242” x 6”) was used as

a *counter electrode* (Figure 13). Carbon rod as a *macroelectrode* was connected to one of the contact pads of the IDE for self induced redox coupling. All the components were assembled in standard configured Gamry eurocell kit (990-00196) item # 13 count 1 (Figure 14a and 14b).

(a) (b)

Figure 11. (a) Saturated calomel electrode (b) Reference electrode bridge tube (Gamry©)

Figure 12. Graphite rod (counter electrode)

(a) (b)

Figure 13. (a) Gamry eurocell (b) Standard configuration of a eurocell (Gamry©)

Different ppm (parts per million) of NH_3 or CO_2 (gases under investigation) with respect to the carrier gas air were fed to the eurocell for noticing the change in electrochemical behavior of the modified IDEs. The ppm values were calculated through the gas flow meters connected to the each gas source. After mixing of the gas under investigation with the carrier gas in the mixing chamber, the obtained ppm value of gas was allowed to pass into the eurocell through gas bubbler assembly (Figure 15). Upon entering into the eurocell this gas gets mixed with the electrolyte and changes its concentration. This change in concentration alters the conductance or resistance value of the chemically modified electrodes and thus results in the change of their electrochemical behavior. This change in electrochemical behavior show corresponding changes in the cyclic voltammograms obtained through cyclic voltammetry that forms the basis of sensor responses. All the electrochemical measurements were carried in 0.1M NaOH electrolyte at a scan rate of 100mV/s (5 cycles each for uniform voltammograms). The cycles were scanned in the potential window range of -1mV to -0.2mV. Figure 16 shows the schematic of the whole electrochemical characterization setup.

Figure 14. Gas bubbler assembly (Gamry©)

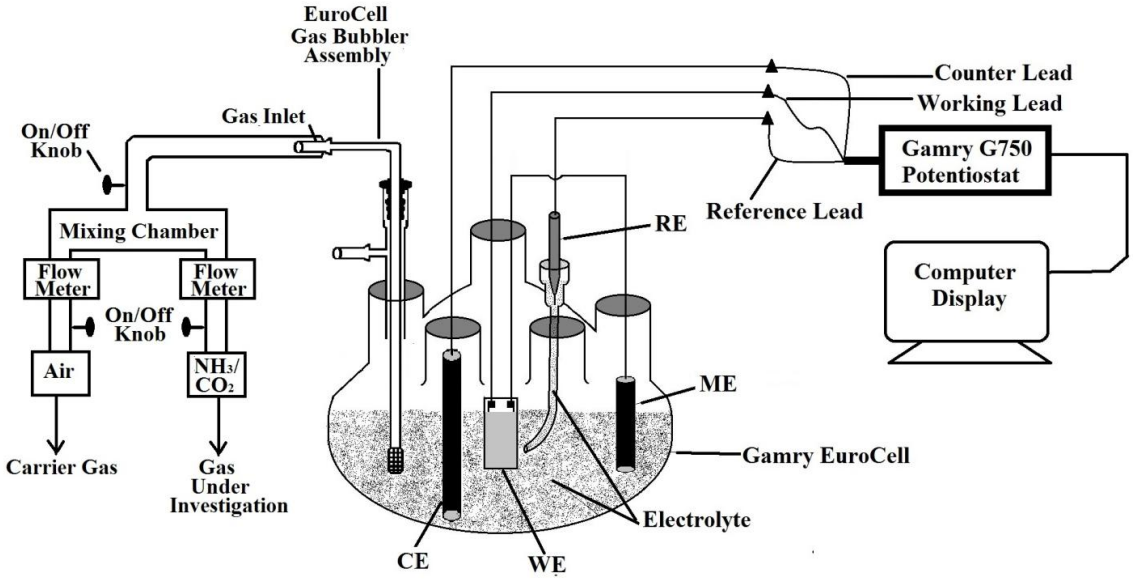

Figure 15. Schematic of the whole electrochemical characterization setup

2.6 Characterization of Sensing Materials

The sensing materials NMF and NMF-rGO were characterized by the following techniques.

2.6.1 X-Ray Diffraction (XRD)

X-ray diffraction analysis was performed by using STOE & Cie GmbH manufactured XRD machine. This machine operated at a current of 40 mA and voltage of 40 KV. The source radiation used was Cu Kα with λ = 0.15418 nm. The 2Θ range for scanning of NMF nanoparticles was kept from 20-80 degrees; while as, for the scanning of NMF-rGO nanocomposite it was kept from 5-70 degrees.

2.6.2 Scanning Electron Microscopy (SEM)

The morphology of NMF nanoparticles and NMF-rGO nanocomposite were investigated by Jeol corporation Japan manufacturer based SEM (model# Jeol JSM-6490A). For SEM analysis, a very little amount from NMFs and NMF-rGO were separately dispersed in two viols having 5ml ultrapure water. These viols were later sonicated for almost 2 hours so that uniform dispersion is achieved. A μL drop from

these dispersions was used in SEM analysis. Since these samples were not conductive, hence a conductive layer of gold coating having approximately 250Å thickness was deposited on them. This was done to enhance the conductivity of the samples. The gold coating was done by using Ion Sputtering machine (JOEL JFC-1500).

Chapter 3

Results and Discussion

3.1 X-Ray Diffraction Analysis of Sensing Materials

Figure 16a shows the XRD analysis plot of NMF nanoparticles between intensity (arbitrary units) on Y-axis and 2Θ (degrees) on X-axis. The XRD pattern of NMF nanoparticles show diffraction lines in the 2Θ range of 20-80^{O}. The XRD pattern shows all the related peaks for the spinel structure and confirms the crystalline structure of NMF nanoparticles that were sintered at 600^{o}C. The broad diffraction peaks in the XRD analysis of NMF nanoparticles show that the synthesized nanoparticles are small in size. The diffraction peaks shown in Figure 15a has matched with the reference pattern JCPDS card no 01-086-2267 for $NiFe_2O_4$ and JCPDS card no 01-073-2410 for $MgFe_2O_4$. The peaks (220), (311), (400), (511) and (440) present in the XRD pattern were found to be well in accordance with these referenced patterns. The crystallite size was calculated by Debye-Scherrer equation using (311) peak and the crystallite size calculated was 10.92 nm. The Debye-Scherrer equation is given as:

$$D = \frac{k\lambda}{\beta cos\theta}$$

Where,

k = constant (0.94)

λ = wavelength of x-ray (wavelength of the source radiation = 1.54060 Å)

β = Full Width Half Maximum (FWHM)

Θ = Half of diffraction angle\

Figure 16b shows the XRD pattern of NMF-rGO nanocomposite in the 2Θ range of 5-70^{O}. The broad diffraction peak visible at 2Θ (25.82) corresponding to the plane (002) shows the presence of rGO peak. In the pattern no GO peak is observed

and the presence of rGO peak shows that the GO has been completely reduced to rGO. The presence of rGO peak confirms the successful synthesis of NMF-rGO nanocomposite.

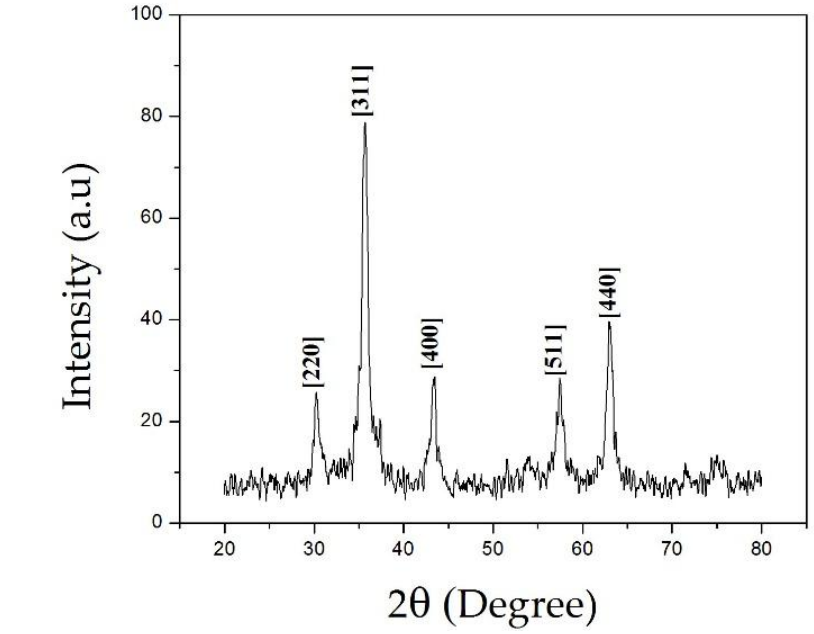

(a)

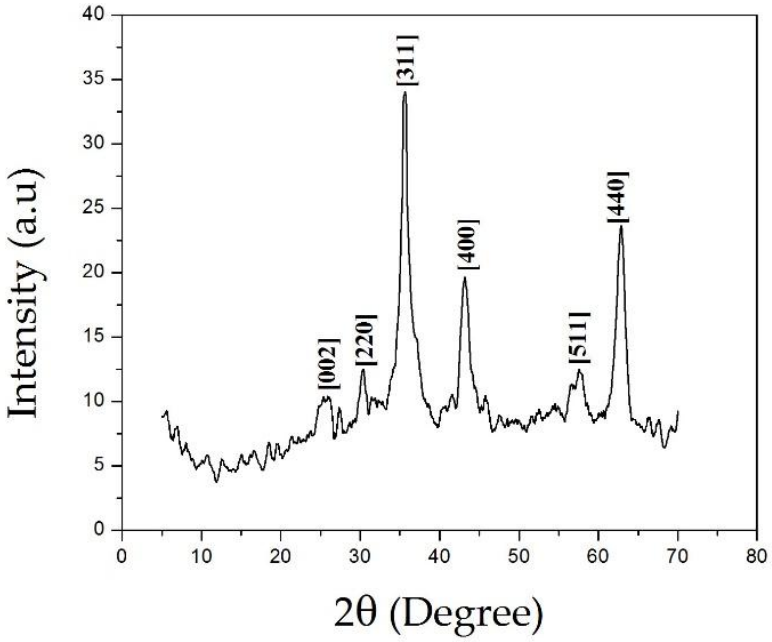

(b)

Figure 16. XRD patterns of (a) NMF nanoparticles (b) NMF-rGO nanocomposite

3.2 Scanning Electron Microscopy of Sensing Materials

Figure 17a shows the SEM image of NMF nanoparticles at X70000 magnification. The analyzed morphology of NMF nanoparticles reveal that the nanoparticles are homogenously well dispersed. The SEM image also confirms the spherical morphology of nanoparticles with the size ranging from 14.20nm to 25.50nm. Figure 17b shows the SEM image of NMF-rGO nanocomposite that reveals spherical NMF nanoparticles are homogenously distributed on graphene sheets. The rGO decorated NMFs confirm the successful synthesis of nanocomposite.

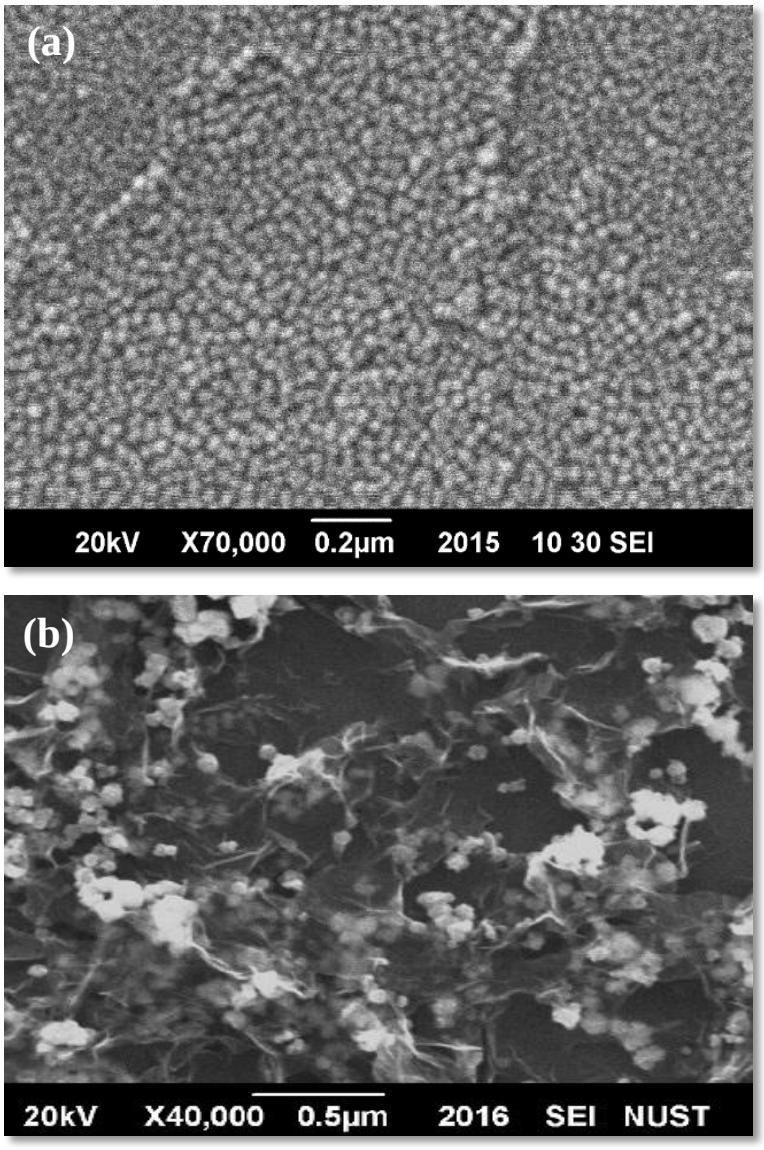

Figure 17. SEM micrographs of (a) NMF nanoparticles (b) NMF-rGO nanocomposite

3.3 Electrochemical Characterization of Chemically Modified Electrodes

The electrochemical characterization of four chemically modified IDEs and a bare IDE (without any modification) has been performed in 0.1M NaOH supporting electrolyte through cyclic voltammetry method. The electrochemical responses of these five types of electrodes have been investigated by exposing them to different concentrations of NH_3 gas. A total of five concentrations 25, 50, 100, 500, 1000ppm of NH_3 have been examined and their respective electrochemical responses have been investigated. Later, the five IDEs were also exposed to 500, 750, 1000, 1250 and 1500ppm concentrations of CO_2 gas so that versatility of the fabricated voltammetric gas sensor could be established.

3.3.1 Electrochemical Response of IDEs in 0.1M NaOH Electrolyte

Figure 18 shows the cyclic voltammograms of bare and modified IDEs in 0.1M NaOH. The minimum current is shown by the bare IDE while the NMF-rGO nanocomposite shows the maximum current. By depositing different sensing materials on the surface of the IDEs, the current increased. In case of NMF nanoparticles current increased due to the increase in surface area of the IDE and its adsorption capability also increased. In case of GO and rGO the current increased due to its conductance changing as a function of extent of surface adsorption, large specific surface area, and low Johnson noise. Charge transfer between the adsorbed molecules and graphene is proposed to be responsible for the chemical response.

As molecules adsorb to the surface of graphene, the location of adsorption experiences a charge transfer with graphene as a donor or acceptor thus changing the Fermi level, carrier density, and electrical resistance of graphene. While, in the case of NMF-rGO nanocomposite; sensor performance in terms of sensitivity is much better as compared to the individual layers of rGO. This is because by combining the NMF with rGO, the electron transfer kinetics, electrode surface area and adsorption capability enhances. So, the combination of NMF and rGO shows up the maximum response. The peak currents (I_p red and I_p ox) and the charge ‘Q’ (Area under the curve) is shown in Table 1.

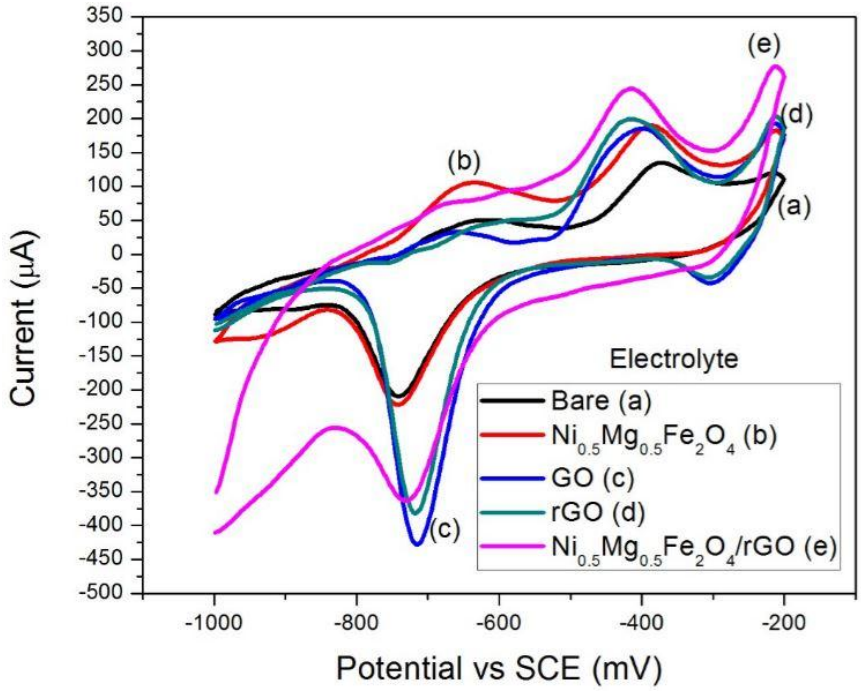

Figure 18. CV curves of the (a) Bare IDEs and (b) NMF (c) GO (d) rGO (e) NMF-rGO modified IDEs in 0.1M NaOH at a scan rate of 100 mV/s.

Table 1. Peak cathodic and anodic currents, Area under the curve (Q) and peak potential separation (ΔEp)

	I_p red (μA)	**-I_p ox (μA)**	**Q (C)**	**ΔEp (V)**
Bare IDE	135.1	209.6	310.2	3.70E-01
NMF IDE	189.6	222.0	544.2	3.56E-01
GO IDE	193.2	427.8	383.7	3.16E-01
rGO IDE	203.1	381.8	419.9	3.02E-01
NMF-rGO IDE	288.7	412.6	598.0	3.16E-01

Table 1 shows the peak reduction current, peak oxidation current, charge (Q) and peak potential separation (ΔEp). The area under the curve (Charge) also increases due to modification the IDEs with nanomaterials. NMF-rGO shows maximum charge due to the fast electron kinetics and more surface area.

3.3.2 Electrochemical Response of IDEs towards 25ppm NH_3 Gas

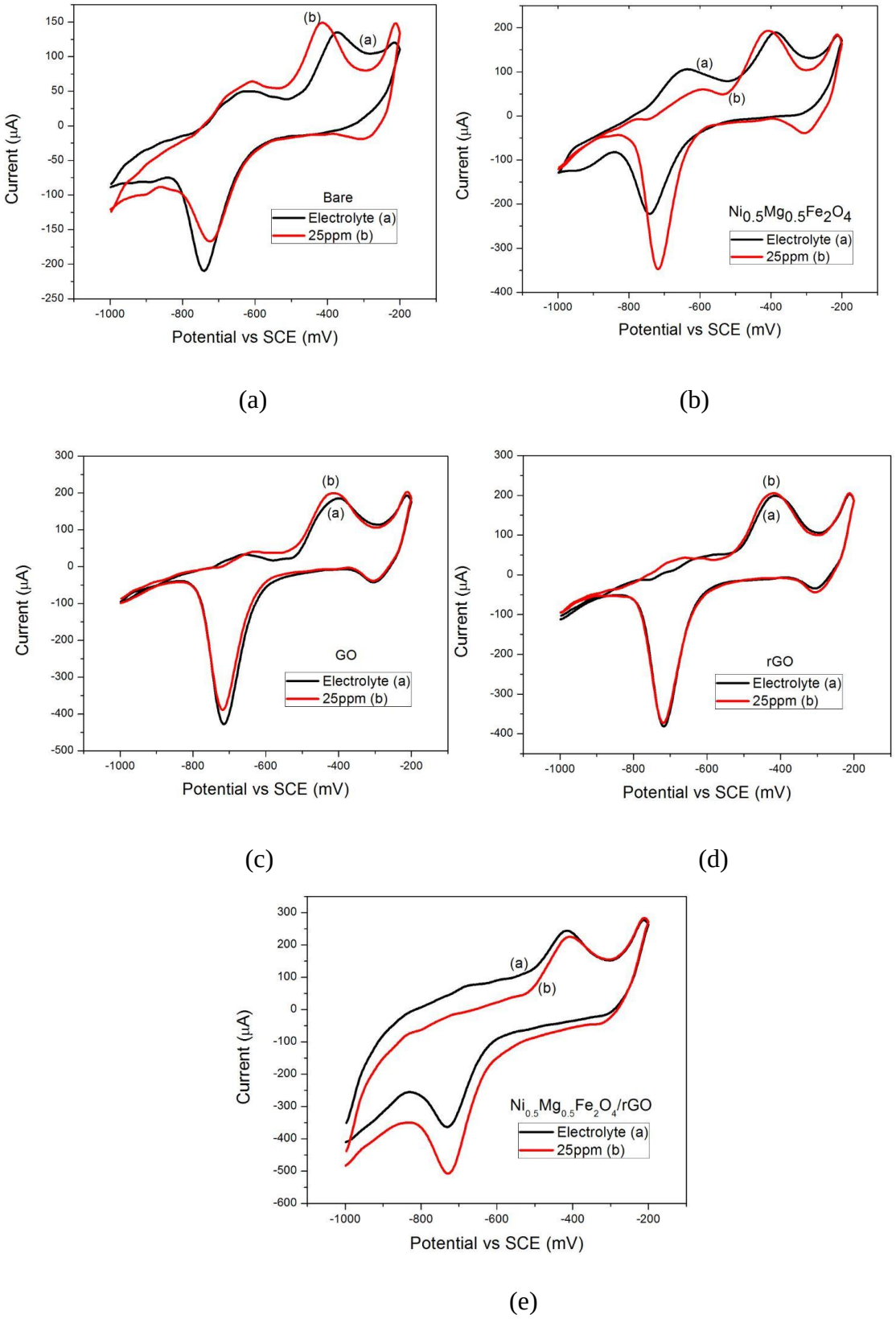

(a) (b)

(c) (d)

(e)

Figure 19. CV curves of (a) bare, (b) NMF, (c) GO, (d) rGO and (e) NMF-rGO IDEs in 0.1M NaOH with and without 25ppm NH_3 gas.

Figure 19 shows the CV responses of bare IDE and chemically modified IDEs in 0.1M NaOH before and after 25ppm NH_3 is purged into the electrolyte. Figure 19a shows response of the bare IDE and minimum current was observed before and after 25ppm NH_3 gas was introduced as compared to the chemically modified IDEs. Figure 19b to 19e shows a considerable increase in current before and after introduction of 25ppm NH_3 as compared to the bare IDE. The maximum current and change was observed in case of NMF-rGO nanocomposite.

Table 2. Current and charge before and after introduction of 25ppm NH_3

	I (µA) (Before NH_3)	**I (µA) (After 25ppm NH_3)**	**Charge (µC) (Before NH_3)**	**Charge (µC) (After 25ppm NH_3)**
Bare IDE	135.1	149.0	310.2	312.2
NMF IDE	189.6	193.2	544.2	404.7
GO IDE	193.2	202.8	383.7	437.5
rGO IDE	203.1	205.7	419.9	455.1
NMF-rGO IDE	288.7	295.8	598.0	221.7

Table 2 shows the change in current and charge before and after introduction of 25ppm NH_3 gas in 0.1M NaOH. The bare and NMF modified IDE does not show any significant change in current; while in case of GO and NMF-rGO nanocomposite, a significant change in current was observed. This shows that a much higher response was obtained by using NMF-rGO nanocomposite.

3.3.3 Electrochemical Response of IDEs towards 50ppm NH_3 Gas

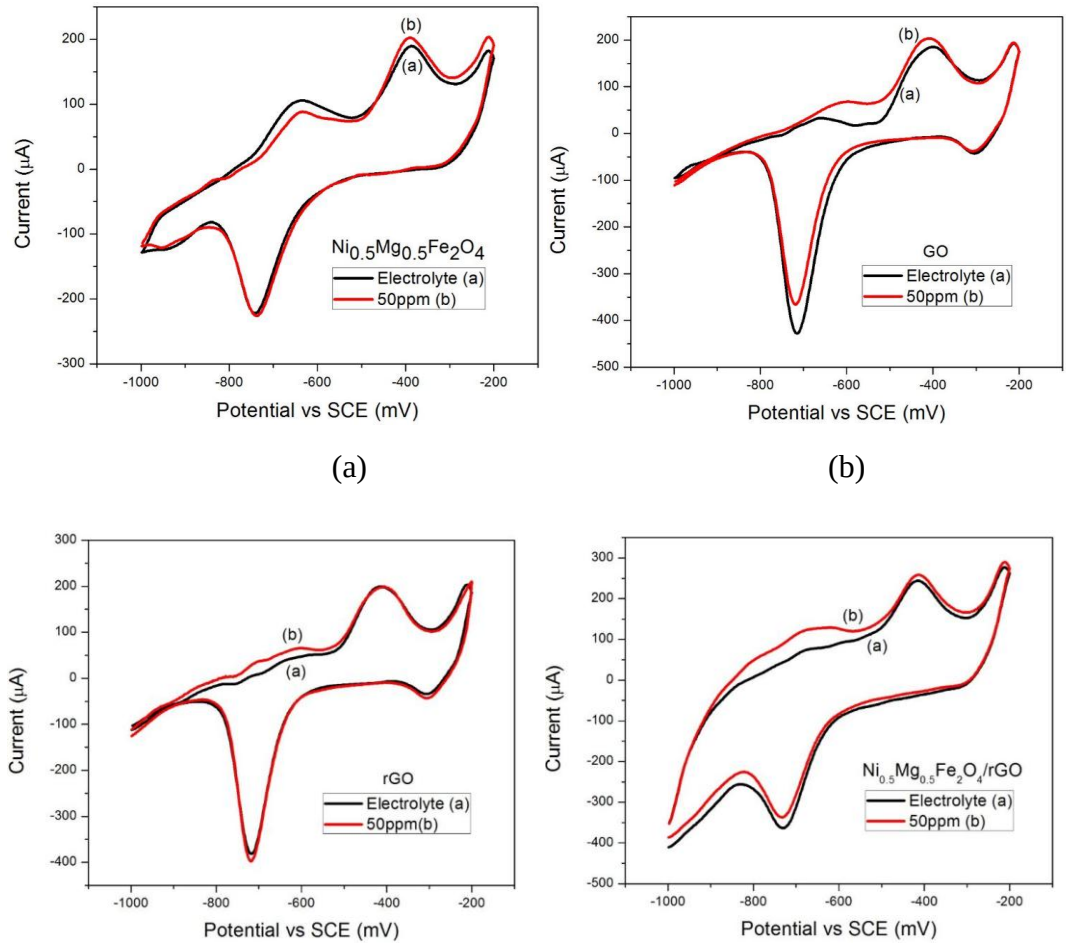

(a) (b)

(c) (d)

Figure 20. CV curves of (a) NMF, (b) GO, (c) rGO and (d) NMF-rGO IDEs in 0.1M NaOH with and without 50ppm NH_3 gas.

Figure 20 shows CV responses of the chemically modified IDEs in 0.1M NaOH before and after 50ppm NH_3 is introduced. By increasing the concentration of NH_3 from 25ppm to 50ppm, a slight increase in current was observed (Table 3). The reasons were already explained in the section 3.3.1.

Table 3. Current and charge before and after introduction of 50ppm NH_3

	I (µA) (Before NH_3)	I (µA) (After 50ppm NH_3)	Charge (µC) (Before NH_3)	Charge (µC) (After 50ppm NH_3)
NMF IDE	189.6	203.6	544.2	541.4
GO IDE	193.2	203.6	383.7	486.8
rGO IDE	203.1	210.7	419.9	478.8
NMF-rGO IDE	288.7	289.9	598.0	775.3

3.3.3 Electrochemical Response of Chemically Modified IDEs towards 100ppm NH_3 Gas

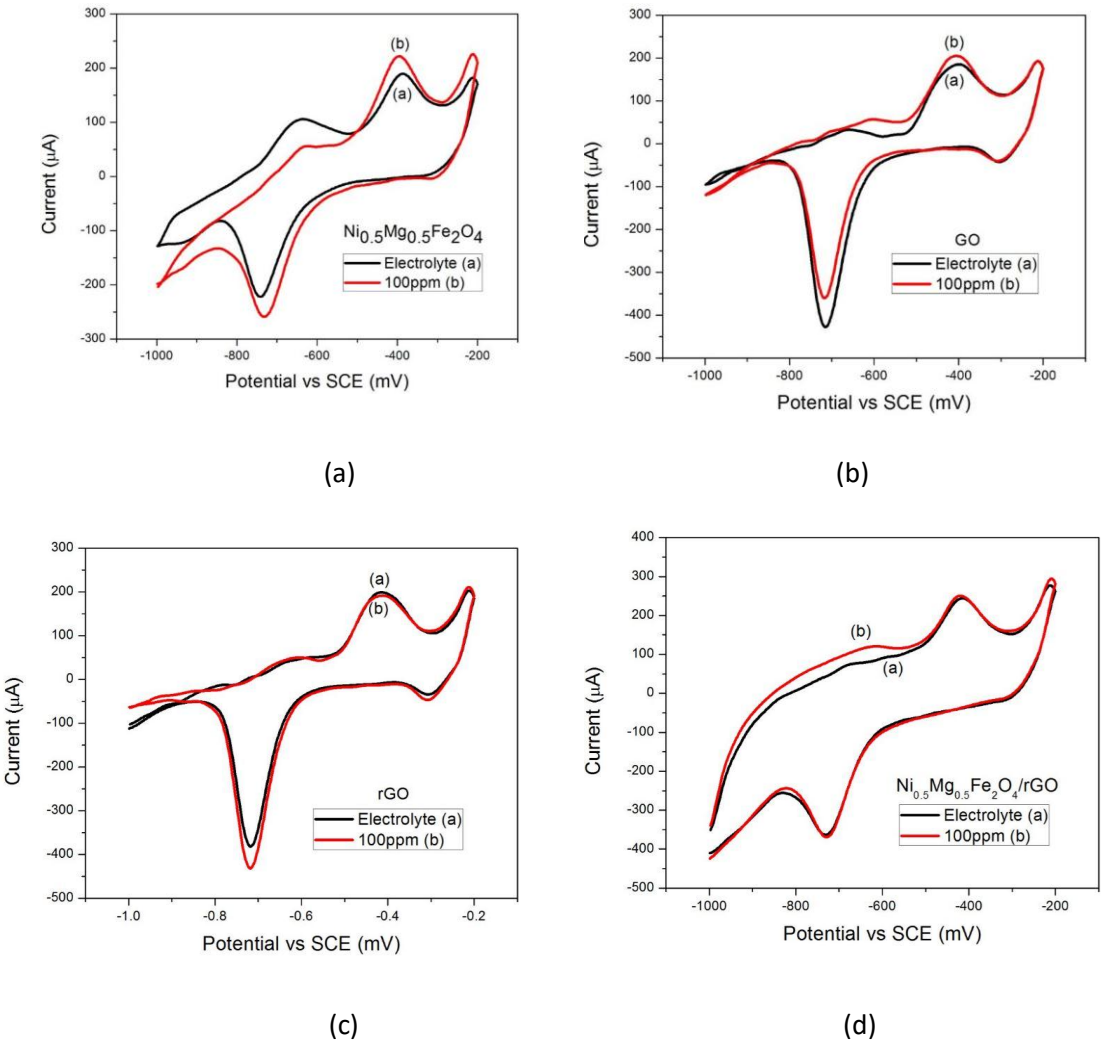

Figure 21. CV curves of (a) NMF, (b) GO, (c) rGO and (d) NMF-rGO IDEs in 0.1M NaOH with and without 100ppm NH_3 gas.

Table 4. Current and charge before and after introduction of 100ppm NH_3

	I (µA) (Before NH_3)	**I (µA) (After 100ppm NH_3)**	**Charge (µC) (Before NH_3)**	**Charge (µC) (After 100ppm NH_3)**
NMF IDE	189.6	226.0	544.2	354.1
GO IDE	193.2	205.3	383.7	448.7
rGO IDE	203.1	211.0	419.9	456.3
NMF-rGO IDE	288.7	294.5	598.0	754.0

3.3.4 Electrochemical Response of Chemically Modified IDEs towards 500ppm NH_3 Gas

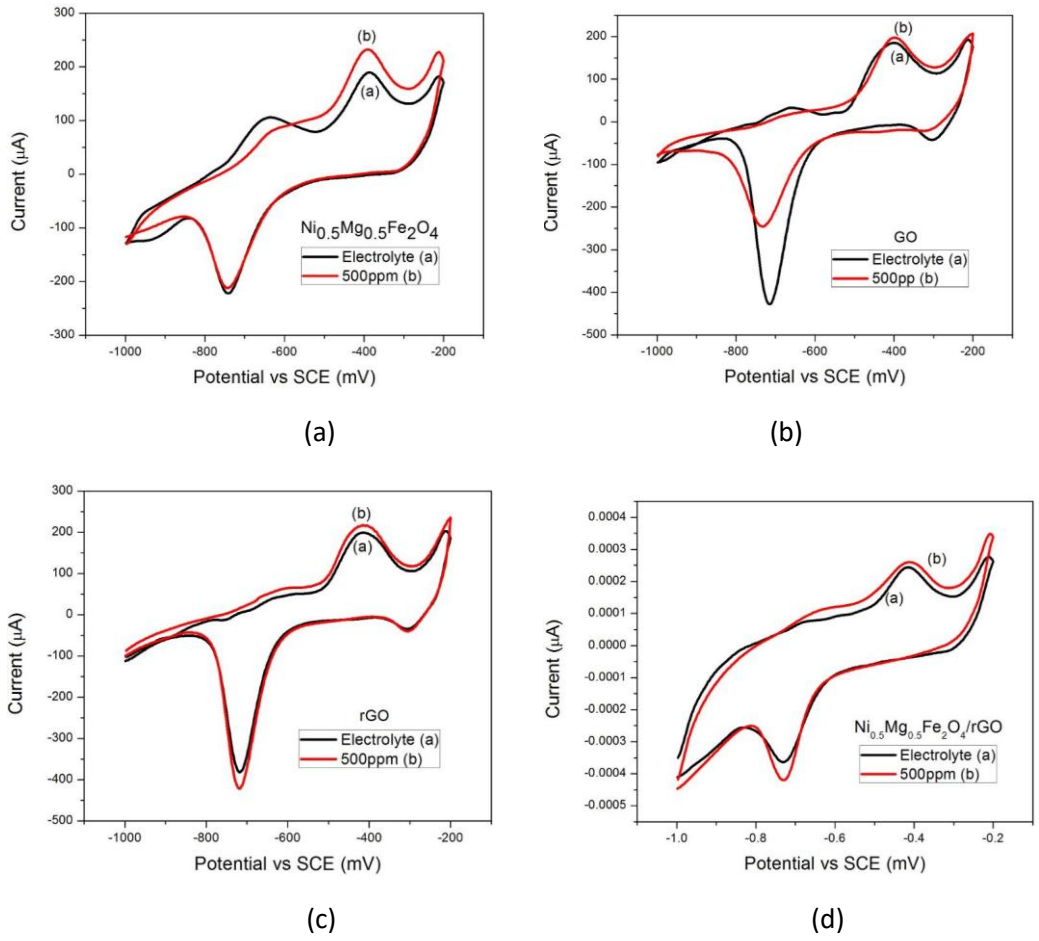

Figure 22. CV curves of (a) NMF, (b) GO, (c) rGO and (d) NMF-rGO IDEs in 0.1M NaOH with and without 500ppm NH_3 gas.

Table 5. Peak current and charge before and after introduction of 500ppm NH_3

	I (µA) (Before NH_3)	**I (µA) (After 500ppm NH_3)**	**Charge (µC) (Before NH_3)**	**Charge (µC) (After 500ppm NH_3)**
NMF IDE	189.6	232.5	544.2	606.7
GO IDE	193.2	207.3	383.7	428.0
rGO IDE	203.1	236.4	419.9	542.5
NMF-rGO	288.7	348.1	598.0	673.0

3.3.5 Electrochemical Response of Chemically Modified IDEs Towards 1000 ppm NH_3 Gas

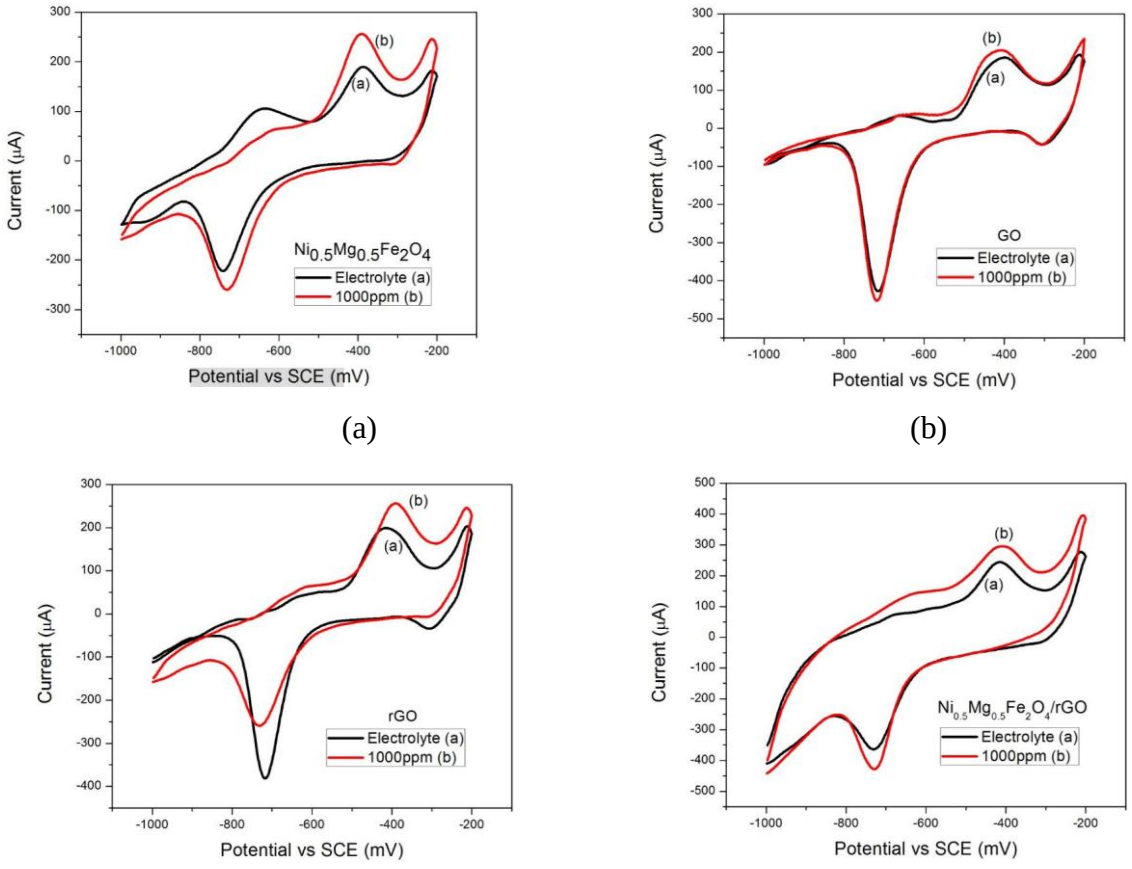

(a) (b)

(c) (d)

Figure 23. CV curves of (a) NMF, (b) GO, (c) rGO and (d) NMF-rGO IDEs in 0.1M NaOH with and without 1000ppm NH_3 gas.

Table 6. Peak current and charge before and after introduction of 1000ppm NH_3

	I (µA) (Before NH_3)	**I (µA) (After 1000ppm NH_3)**	**Charge (µC) (Before NH_3)**	**Charge µ(C) (After 1000ppm NH_3)**
NMF IDE	189.6	256.3	544.2	543.8
GO IDE	193.2	234.8	383.7	471.2
rGO IDE	203.1	256.3	419.9	543.8
NMF-rGO IDE	288.7	395.9	598.0	903.4

3.3.6 Calibration Curve for Different Concentrations of NH_3

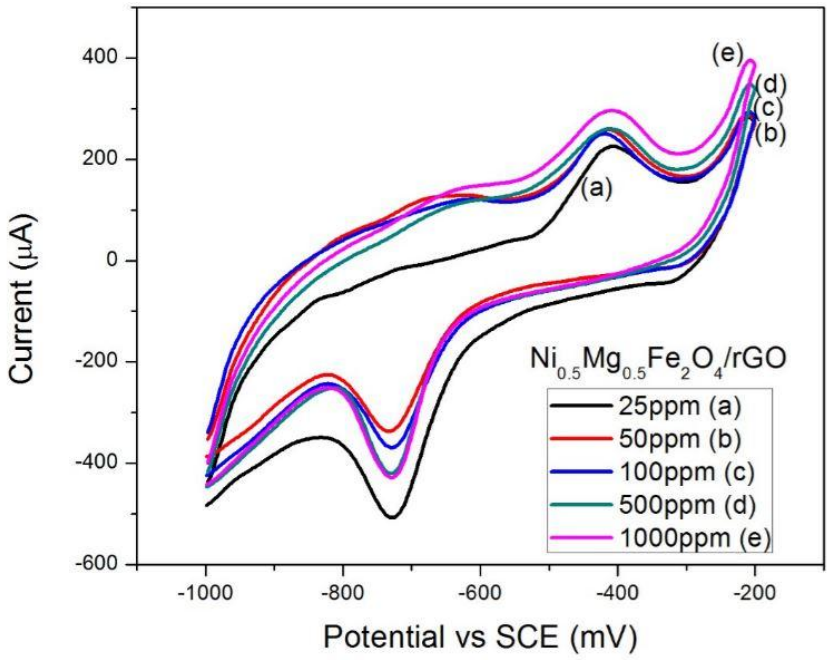

(a)

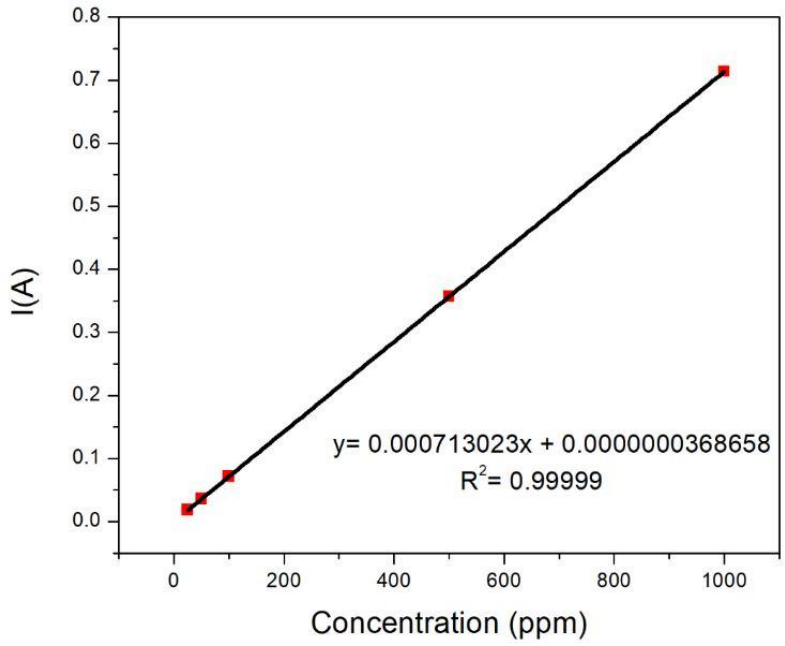

(b)

Figure 24. (a) CV curves of NMF-rGO modified IDEs exposed to 25-1000 ppm concentrations of NH_3 (b) Calibration curve of the NMF-rGO modified IDE over a concentration range from 25-1000 ppm.

Calibration curve is used to find the limit of detection (LOD) and the sensitivity of a sensor. Since, NMF-rGO modified IDE showed improved electrochemical response to all the concentrations of NH_3; hence only NMF-rGO voltammograms were compared to plot the calibration curve. Figure 24b shows the calibration plot of the CV curves of NMF-rGO nanocomposite modified IDEs exposed to a concentration range of 25-1000ppm NH_3 gas (Figure 24a). The linearization equation was found to be y=0.000713023x+0.0000000368658, with correlation coefficient of 0.99999.

LOD was calculated using 3Ʊ (3 sigma) method as given:

$$\textbf{LOD} = \frac{\textbf{3.3*Standard Deviation}}{\textbf{Slope}}$$

Analysis tool in the origin software was used to calculate the parameters of the calibration curve as shown in Table 7. The value of LOD calculated by 3 sigma method was found to be 17.1 ppm. The sensitivity of the sensor was calculated from

the slope of the calibration curve (current v/s concentration), which in this case is 0.000713023 A ppm^{-1}.

Table 7. Parameters of the calibration curve

	Value	Standard Error
Intercept	3.38393E-4	3.68658E-8
Slope	7.13023E-4	7.33475E-11

.

3.3.7 Electrochemical Response of IDEs Towards 500ppm CO_2 Gas

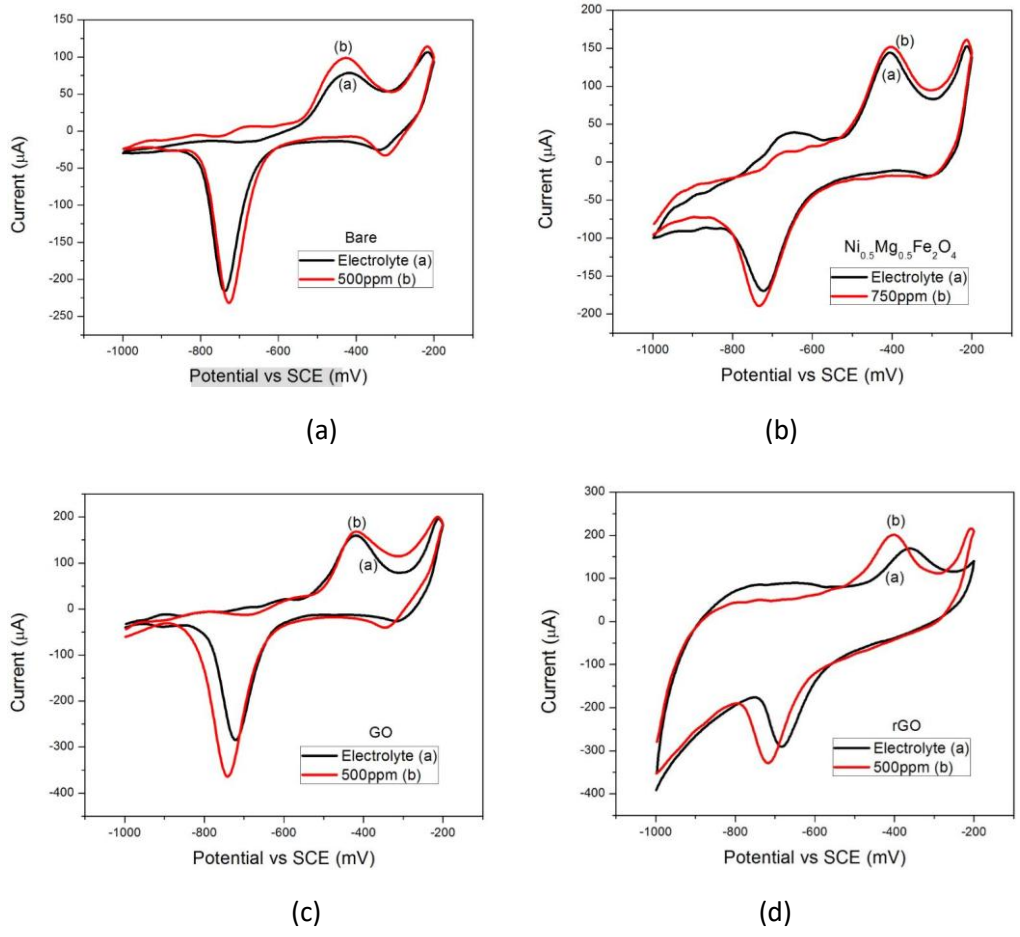

(a) (b)

(c) (d)

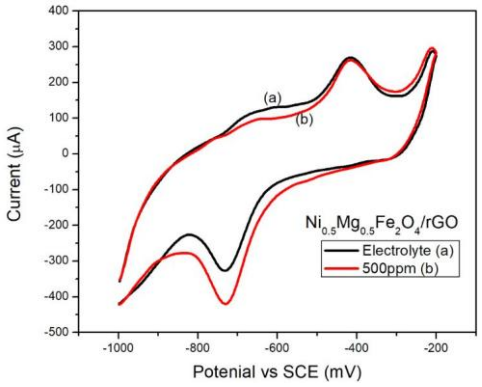

(e)

Figure 25. CV curves of (a) bare, (b) NMF, (c) GO, (d) rGO and (e) NMF-rGO IDEs in 0.1M NaOH with and without 500ppm CO_2 gas

Figure 25 shows the CV responses of a bare IDE and chemically modified IDEs in 0.1M NaOH before and after purging of 500ppm CO_2 in it. Similar trend was noticed in the responses of differently treated IDEs as was found during NH_3 gas investigation. Current increased due to the purging of 500ppm CO_2 into 0.1M NaOH electrolyte as is evident from the CV graphs in Figure 25a to 25e. The current and charge data collected from the CV curves is shown in Table 8.

Table 8. Current and charge before and after introduction of 500ppm CO_2

	I (μA) (Before CO_2)	**I (μA) (After 500ppm CO_2)**	**Charge (μC) (Before CO_2)**	**Charge (μC) (After 500ppm CO_2)**
Bare IDE	78.29	99.62	155.1	234.2
NMF IDE	151.6	144.2	304.5	286.0
GO IDE	159.7	168.5	358.8	387.3
rGO IDE	169.3	201.2	544.7	540.9
NMF-rGO IDE	269.9	266.0	732.4	689.0

3.3.8 Electrochemical Response of Chemically Modified IDEs Towards 750ppm CO_2 Gas

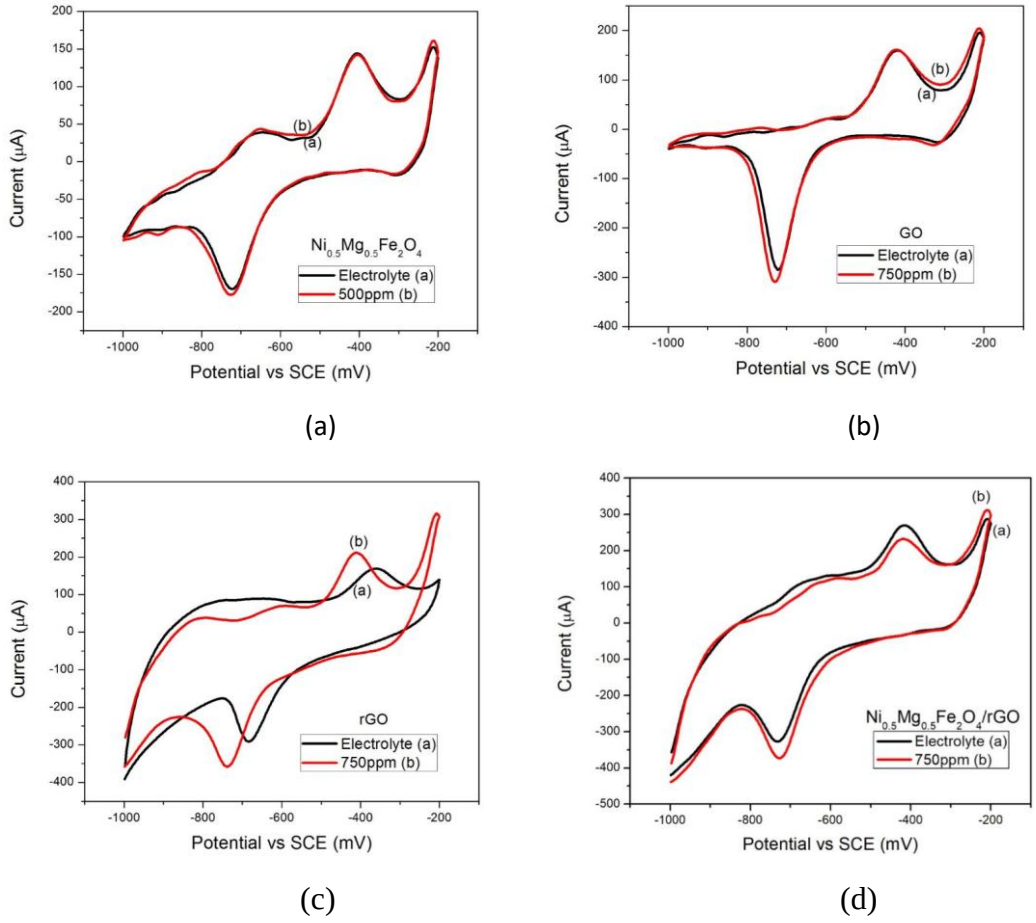

Figure 26. CV curves of (a) NMF, (b) GO, (c) rGO and (d) NMF-rGO IDEs in 0.1M NaOH with and without 750ppm CO_2 gas.

CV responses of the modified IDEs were used for the detection of 750ppm CO_2 in 0.1M NaOH (Figure 26). By increasing the concentration of carbon dioxide from 500ppm to 750ppm, increase in current was observed. The reasons have already been explained.

Table 9. Current and charge before and after introduction of 750ppm CO_2

	I (μA) (Before CO_2)	**I (μA) (After 750ppm CO_2)**	**Charge (μC) (Before CO_2)**	**Charge μ(C) (After 750ppm CO_2)**
NMF IDE	151.6	142.0	304.5	303.1

GO IDE	159.7	161.3	358.8	400.4
rGO IDE	169.3	211.0	544.7	533.5
NMF-rGO IDE	269.9	232.1	732.4	647.4

3.3.9 Electrochemical Response of Chemically Modified IDEs Towards 1000 ppm CO_2 Gas

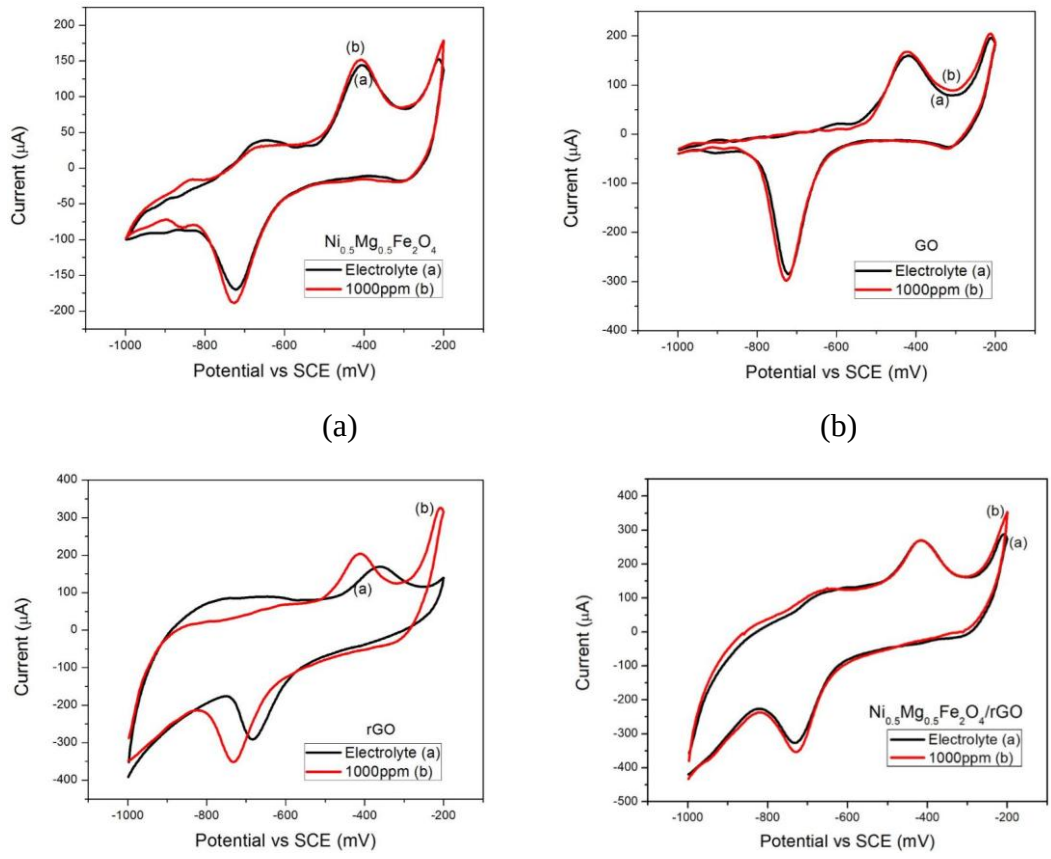

(a) (b)

(c) (d)

Figure 27. CV curves of (a) NMF, (b) GO, (c) rGO and (d) NMF-rGO IDEs in 0.1M NaOH with and without 1000ppm CO_2 gas.

Table 10. Current and charge before and after introduction of 1000ppm CO_2

	I (µA) (Before CO_2)	I (µA) (After 1000ppm CO_2)	Charge (µC) (Before CO_2)	Charge (µC) (After 1000ppm CO_2)
NMF IDE	151.6	151.8	304.5	312.5
GO IDE	159.7	167.8	358.8	372.2
rGO IDE	169.3	203.6	544.7	567.4
NMF-rGO IDE	269.9	270.2	732.4	811.4

3.3.10 Electrochemical Response of Chemically Modified IDEs Towards 1250 ppm CO_2 Gas

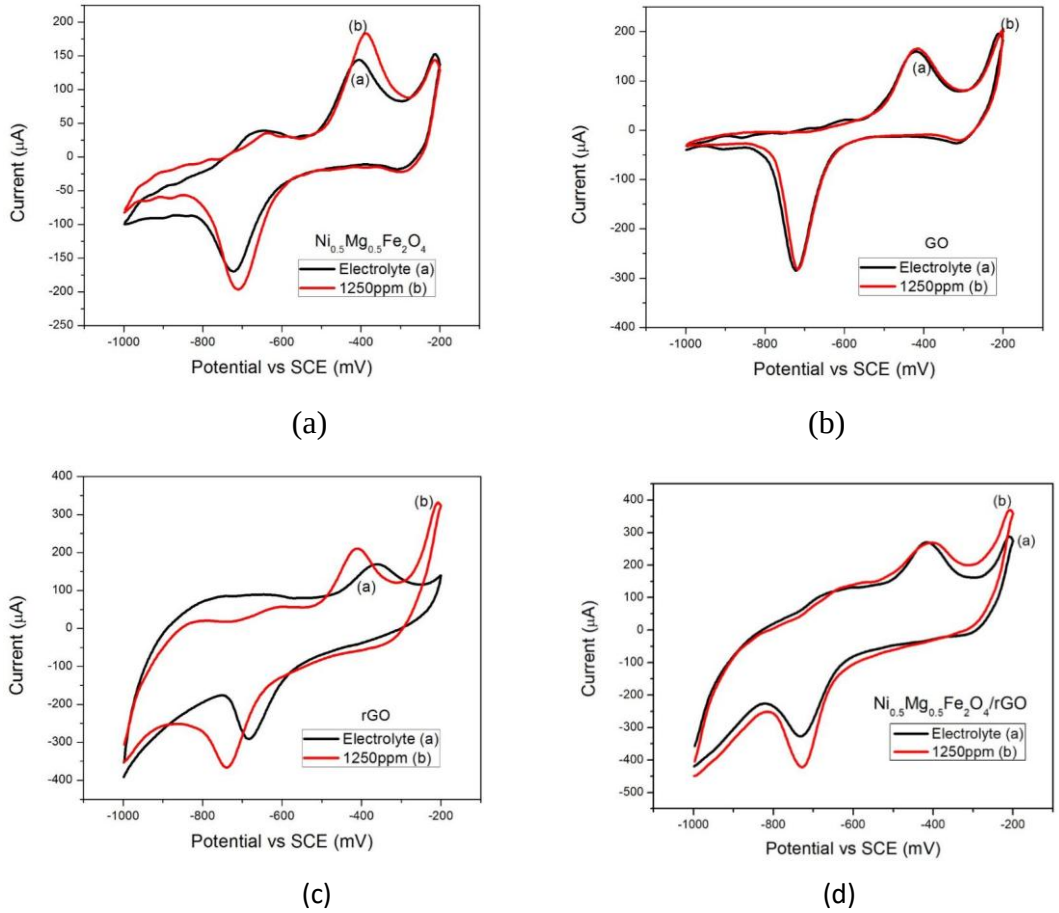

(a) (b)

(c) (d)

Figure 28. CV curves of (a) NMF, (b) GO, (c) rGO and (d) NMF-rGO IDEs in 0.1M NaOH with and without 1250ppm CO_2 gas.

Table 11. Current and charge before and after introduction of 1250ppm CO_2

	I (µA) (Before CO_2)	I (µA) (After 1250ppm CO_2)	Charge (µC) (Before CO_2)	Charge (µC) (After 1250ppm CO_2)
NMF IDE	151.6	172.1	304.5	347.0
GO IDE	159.7	165.5	358.8	262.2
rGO IDE	169.3	210.4	544.7	481.9
NMF-rGO IDE	269.9	268.6	732.4	797.8

3.3.11 Electrochemical Response of Chemically Modified IDEs Towards 1500 ppm CO_2 Gas

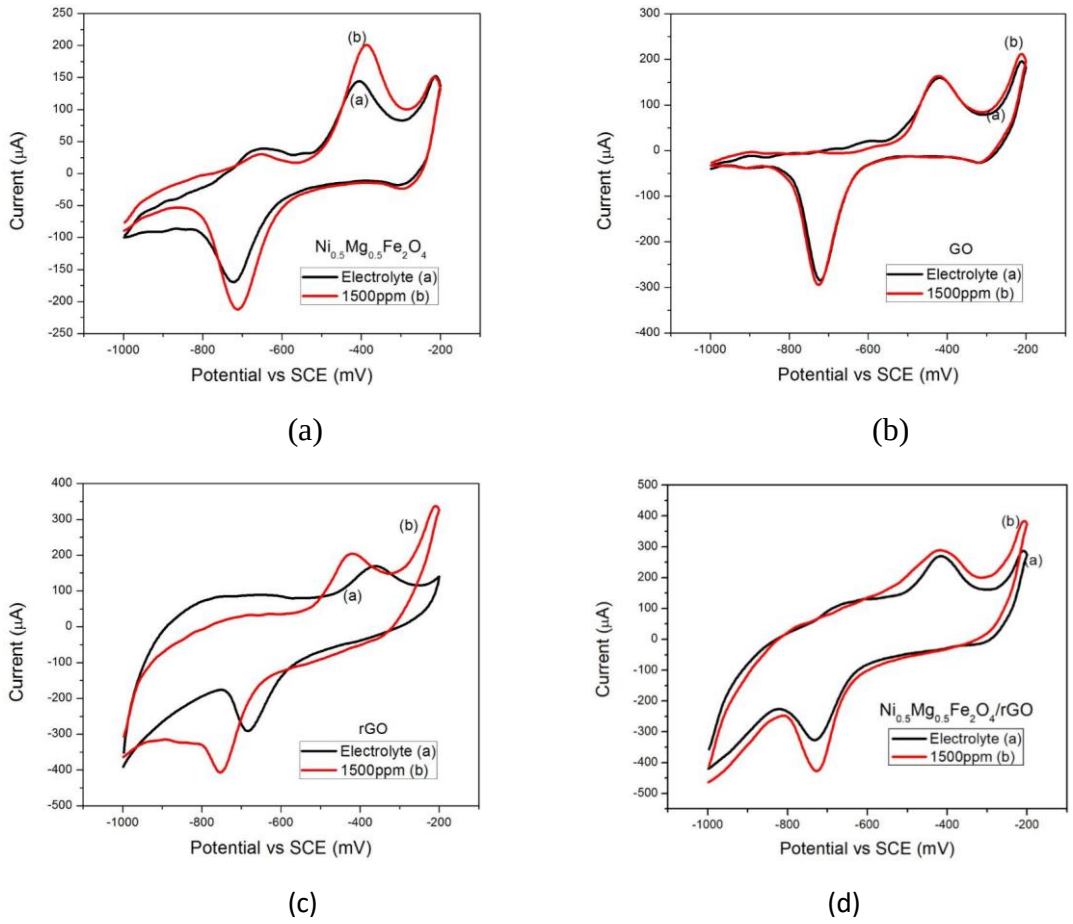

Figure 29. CV curves of (a) NMF, (b) GO, (c) rGO and (d) NMF-rGO IDEs in 0.1M NaOH with and without 1500ppm CO_2 gas.

Table 12. Current and charge before and after introduction of 1500ppm CO_2

	I (µA) (Before CO_2)	**I (µA) (After 1500ppm CO_2)**	**Charge (µC) (Before CO_2)**	**Charge (µC) (After 1500ppm CO_2)**
NMF IDE	151.6	205.2	304.5	380.7
GO IDE	159.7	163.8	358.8	363.2
rGO IDE	169.3	204.1	544.7	474.5
NMF-rGO	269.9	290.6	732.4	803.2

Chapter 4

Conclusions

In this study, a simple and low cost process was demonstrated to quickly fabricate copper based interdigitated electrodes with good electrochemical performance. The changes in cyclic voltammetric response and current values of differently treated IDEs indicate that these electrodes can be used for sensor studies. It has been observed that the surface of used IDEs can be activated again for re-use by gently scrubbing with ultrafine sand paper; followed by cleaning with ethanol and ultrapure water. However, after each cleaning process almost 0.005mm of copper electrode material gets removed but the electrochemical performance remains mostly stable. Storage in air tight chamber is required to prevent the IDE surface from gathering an oxide layer that affects the electrochemical performance. The dimensions of IDEs can be further decreased if the PVC ink used for design formation is handled precisely. This fabrication process, applied to copper boards readily available in electronics market, can also be applied to aluminium coated substrates (glass, fiber etc.,) to fabricate aluminium based IDEs. Less manual operation is required to minimize unnecessary faults and obviously more study is needed to understand more details about this simple technique.

Various nanomaterials having sensing capabilities were synthesized. Co-precipitation route has been employed to synthesize nickel magnesium ferrite ($Ni_{0.5}Mg_{0.5}Fe_2O_4$). Literature suggested that various spinel ferrites have already been investigated for their sensing capabilities. The nanocomposite of $Ni_{0.5}Mg_{0.5}Fe_2O_4$ with reduced graphene oxide (rGO) has been obtained through physical method by ultrasonication technique. Powder XRD and SEM techniques were used to study the morphological and structural properties of these sensing materials. The SEM results of $Ni_{0.5}Mg_{0.5}Fe_2O_4$ nanoparticles confirmed the spherical morphology of nanoparticles with the average particle size to be 20nm and no agglomeration was observed. The SEM micrograph of nanocomposite showed that these spherical $Ni_{0.5}Mg_{0.5}Fe_2O_4$ nanoparticles are homogenously distributed on graphene sheets. The

XRD results showed that all the relevant peaks are present, thus justifying the formation of required sensing materials.

The four types of sensing materials i.e., $Ni_{0.5}Mg_{0.5}Fe_2O_4$ nanoparticles, GO, rGO and $Ni_{0.5}Mg_{0.5}Fe_2O_4$-rGO nanocomposite were used to chemically modify different IDEs. These chemically modified IDEs acted as voltammetric sensors and their sensing capabilities were examined by electrochemical characterization through cyclic voltammetry. These voltammetric sensors when exposed to different concentrations of NH_3 and CO_2 gases in 0.1M NaOH electrolyte showed considerable responses in the form of change in current. The cyclic voltammograms obtained reveal that all the modified IDEs show considerable change in peak currents with and without the presence of gas (analyte) concentration in the electrolyte. The maximum response towards various gas concentrations of NH_3 and CO_2 was shown by the $Ni_{0.5}Mg_{0.5}Fe_2O_4$/rGO nanocomposite modified IDE while as bare electrode showed very limited change in the response followed by $Ni_{0.5}Mg_{0.5}Fe_2O_4$ nanoparticles modified IDE. The sensitivity and limit of detection (LOD) of $Ni_{0.5}Mg_{0.5}Fe_2O_4$/rGO nanocomposite modified IDE towards various concentrations of NH_3 gas have been calculated. The sensitivity achieved by using $Ni_{0.5}Mg_{0.5}Fe_2O_4$/rGO nanocomposite as a sensing element was found to be 0.000713023 A ppm^{-1} and limit of detection (LOD) obtained was 17.1 ppm, which is below the threshold limit of 25ppm set by the world health organization (WHO).

It can be concluded that the copper based IDEs when modified with various sensing nanomaterials coating show a promising use as electrochemical sensors but this research area needs further tuning so that more robust, re-usable and selective electrochemical sensor could be developed.

References

[1] J. Janata, Peer Reviewed: Centennial Retrospective on Chemical Sensors, ACS Publications2001.
[2] J.R. Stetter, W.R. Penrose, S. Yao, Sensors, chemical sensors, electrochemical sensors, and ECS, Journal of The Electrochemical Society, 150(2003) S11-S6.
[3] F. Yi, D.A. La Van, Nanoscale thermal analysis for nanomedicine by nanocalorimetry, Wiley Interdisciplinary Reviews: Nanomedicine and Nanobiotechnology, 4(2012) 31-41.
[4] J.N. Anker, W.P. Hall, O. Lyandres, N.C. Shah, J. Zhao, R.P. Van Duyne, Biosensing with plasmonic nanosensors, Nature materials, 7(2008) 442-53.
[5] P.S. Waggoner, H.G. Craighead, Micro-and nanomechanical sensors for environmental, chemical, and biological detection, Lab on a Chip, 7(2007) 1238-55.
[6] A.C. Power, A. Morrin, Electroanalytical sensor technology: INTECH Open Access Publisher; 2013.
[7] N.R. Stradiotto, H. Yamanaka, M.V.B. Zanoni, Electrochemical sensors: a powerful tool in analytical chemistry, Journal of the Brazilian Chemical Society, 14(2003) 159-73.
[8] J. Janata, Principles of chemical sensors: Springer Science & Business Media; 2010.
[9] A. Gildea, Electrochemical Sensors.
[10] J. Li, Y. Lu, A highly sensitive and selective catalytic DNA biosensor for lead ions, Journal of the American Chemical Society, 122(2000) 10466-7.
[11] M.A. Khan, F. Qazi, Z. Hussain, M.U. Idrees, S. Soomro, S. Soomro, Recent Trends in Electrochemical Detection of NH3, H2S and NOx Gases, INTERNATIONAL JOURNAL OF ELECTROCHEMICAL SCIENCE, 12(2017) 1711-33.
[12] J. Wang, K. Rogers, Electrochemical sensors for environmental monitoring: a review of recent technology: US Environmental Protection Agency, Office of Research and Development, Environmental Monitoring and Support Laboratory; 1995.
[13] D. Diamond, F. Collins, J. Cleary, C. Zuliani, C. Fay, Distributed environmental monitoring, Autonomous Sensor Networks, Springer2012, pp. 321-63.
[14] D.A. Skoog, D.M. West, F.J. Holler, S. Crouch, Fundamentals of analytical chemistry: Nelson Education; 2013.
[15] P. Kissinger, W.R. Heineman, Laboratory Techniques in Electroanalytical Chemistry, revised and expanded: CRC press; 1996.
[16] A.J. Bard, L.R. Faulkner, J. Leddy, C.G. Zoski, Electrochemical methods: fundamentals and applications: wiley New York; 1980.
[17] C.G. Zoski, Handbook of electrochemistry: Elsevier; 2006.
[18] D. Skoog, D. West, F. Holler, Fundamentals of analytical chemistry Saunders College Pub, Fort Worth, (1992).
[19] A. Álvarez-Lueje, M. Pérez, C. Zapata, Electrochemical methods for the in vitro assessment of drug metabolism, Topics on Drug Metabolism, InTech2012.
[20] N. Agbor, M. Petty, A. Monkman, Polyaniline thin films for gas sensing, Sensors and Actuators B: Chemical, 28(1995) 173-9.
[21] G. Li, C. Martinez, S. Semancik, Controlled electrophoretic patterning of polyaniline from a colloidal suspension, Journal of the American Chemical Society, 127(2005) 4903-9.
[22] H. Yoon, M. Chang, J. Jang, Sensing behaviors of polypyrrole nanotubes prepared in reverse microemulsions: effects of transducer size and transduction mechanism, The Journal of Physical Chemistry B, 110(2006) 14074-7.
[23] D. Liu, J. Aguilar-Hernandez, K. Potje-Kamloth, H. Liess, A new carbon monoxide sensor using a polypyrrole film grown on an interdigital-capacitor substrate, Sensors and Actuators B: Chemical, 41(1997) 203-6.

[24] E.O. Barnes, G.E. Lewis, S.E. Dale, F. Marken, R.G. Compton, Generator-collector double electrode systems: A review, Analyst, 137(2012) 1068-81.
[25] O. Niwa, Electroanalysis with interdigitated array microelectrodes, Electroanalysis, 7(1995) 606-13.
[26] K. Ueno, M. Hayashida, J.-Y. Ye, H. Misawa, Fabrication and electrochemical characterization of interdigitated nanoelectrode arrays, Electrochemistry communications, 7(2005) 161-5.
[27] L. Löfgren, B. Löfving, T. Pettersson, B. Ottosson, C. Rusu, S. Haasl, et al., Low-power humidity sensor for RFID applications, Whittles Publishing, Cardiff2008.
[28] K.-S. Chou, C.-H. Lee, Fabrication of silver interdigitated electrode by a stamp method, Advances in Materials Science and Engineering, 2014(2014).
[29] U. Hashim, A. Puah, C. Voon, M.M. Arshad, W.-W. Liu, S. Kahar, et al., Low cost mask layout design for fabrication of spiral interdigitated electrodes in electrochemical biosensor application, Biomedical Engineering (ICoBE), 2015 2nd International Conference on, IEEE2015, pp. 1-5.
[30] L. Bueno, T.R. Paixao, A copper interdigitated electrode and chemometrical tools used for the discrimination of the adulteration of ethanol fuel with water, Talanta, 87(2011) 210-5.
[31] D.D. Le, T.N.N. Nguyen, D.C.T. Doan, T.M.D. Dang, M.C. Dang, Fabrication of interdigitated electrodes by inkjet printing technology for apllication in ammonia sensing, Advances in Natural Sciences: Nanoscience and Nanotechnology, 7(2016) 025002.
[32] A.J. Bard, Chemical modification of electrodes, ACS Publications1983.
[33] M. Musameh, J. Wang, A. Merkoci, Y. Lin, Low-potential stable NADH detection at carbon-nanotube-modified glassy carbon electrodes, Electrochemistry Communications, 4(2002) 743-6.
[34] C.E. Banks, T.J. Davies, G.G. Wildgoose, R.G. Compton, Electrocatalysis at graphite and carbon nanotube modified electrodes: edge-plane sites and tube ends are the reactive sites, Chemical Communications, (2005) 829-41.
[35] V.A. Kumary, J. Divya, T.M. Nancy, K. Sreevalsan, Voltammetric detection of paracetamol at cobalt ferrite nanoparticles modified glassy carbon electrode, Int J Electrochem Sci, 8(2013) 6610-9.
[36] A. Abbaspour, E. Mirahmadi, Electrocatalytic hydrogen evolution reaction on carbon paste electrode modified with Ni ferrite nanoparticles, Fuel, 104(2013) 575-82.
[37] W.R. Heineman, H.J. Wieck, A.M. Yacynych, Polymer film chemically modified electrode as a potentiometric sensor, Analytical Chemistry, 52(1980) 345-6.
[38] M.M. Barsan, M.E. Ghica, C.M. Brett, Electrochemical sensors and biosensors based on redox polymer/carbon nanotube modified electrodes: A review, Analytica chimica acta, 881(2015) 1-23.
[39] F. Wang, L. Zhu, J. Zhang, Electrochemical sensor for levofloxacin based on molecularly imprinted polypyrrole–graphene–gold nanoparticles modified electrode, Sensors and Actuators B: Chemical, 192(2014) 642-7.
[40] S. Koçak, B. Aslışen, Hydrazine oxidation at gold nanoparticles and poly (bromocresol purple) carbon nanotube modified glassy carbon electrode, Sensors and Actuators B: Chemical, 196(2014) 610-8.
[41] L. Yang, D. Liu, J. Huang, T. You, Simultaneous determination of dopamine, ascorbic acid and uric acid at electrochemically reduced graphene oxide modified electrode, Sensors and Actuators B: Chemical, 193(2014) 166-72.
[42] C. Wang, J. Du, H. Wang, C.e. Zou, F. Jiang, P. Yang, et al., A facile electrochemical sensor based on reduced graphene oxide and Au nanoplates modified glassy carbon electrode for simultaneous detection of ascorbic acid, dopamine and uric acid, Sensors and Actuators B: Chemical, 204(2014) 302-9.

[43] N. Aristov, A. Habekost, Cyclic voltammetry-A versatile electrochemical method investigating electron transfer processes, World Journal of Chemical Education, 3(2015) 115-9.
[44] J.F. Rusling, S.L. Suib, Characterizing materials with cyclic voltammetry, Advanced Materials, 6(1994) 922-30.
[45] N.G. Tsierkezos, Cyclic voltammetric studies of ferrocene in nonaqueous solvents in the temperature range from 248.15 to 298.15 K, Journal of Solution Chemistry, 36(2007) 289-302.
[46] F. Zhao, R.C. Slade, J.R. Varcoe, Techniques for the study and development of microbial fuel cells: an electrochemical perspective, Chemical Society Reviews, 38(2009) 1926-39.
[47] S.-K. Lee, D. Chang, S.W. Kim, Gas sensors based on carbon nanoflake/tin oxide composites for ammonia detection, Journal of hazardous materials, 268(2014) 110-4.
[48] S.P. Basak, B. Kanjilal, P. Sarkar, A.P. Turner, Application of electrical impedance spectroscopy and amperometry in polyaniline modified ammonia gas sensor, Synthetic metals, 175(2013) 127-33.
[49] J. Oudenhoven, W. Knoben, R. van Schaijk, Electrochemical Detection of Ammonia Using a Thin Ionic Liquid Film as the Electrolyte, Procedia Engineering, 120(2015) 983-6.
[50] Y. Li, H. Ban, M. Yang, Highly sensitive NH3 gas sensors based on novel polypyrrole-coated SnO2 nanosheet nanocomposites, Sensors and Actuators B: Chemical, 224(2016) 449-57.
[51] S. Xu, K. Kan, Y. Yang, C. Jiang, J. Gao, L. Jing, et al., Enhanced NH3 gas sensing performance based on electrospun alkaline-earth metals composited SnO2 nanofibers, Journal of Alloys and Compounds, 618(2015) 240-7.
[52] J. Deng, R. Zhang, L. Wang, Z. Lou, T. Zhang, Enhanced sensing performance of the Co3O4 hierarchical nanorods to NH3 gas, Sensors and Actuators B: Chemical, 209(2015) 449-55.
[53] B. Wu, L. Wang, H. Wu, K. Kan, G. Zhang, Y. Xie, et al., Templated synthesis of 3D hierarchical porous Co3O4 materials and their NH3 sensor at room temperature, Microporous and Mesoporous Materials, 225(2016) 154-63.
[54] Y. Lin, K. Kan, W. Song, G. Zhang, L. Dang, Y. Xie, et al., Controllable synthesis of Co3O4/polyethyleneimine-carbon nanotubes nanocomposites for CO and NH3 gas sensing at room temperature, Journal of Alloys and Compounds, 639(2015) 187-96.
[55] L. Dai, G. Yang, H. Zhou, Z. He, Y. Li, L. Wang, Mixed potential NH3 sensor based on Mg-doped lanthanum silicate oxyapatite, Sensors and Actuators B: Chemical, 224(2016) 356-63.
[56] W. Meng, L. Dai, J. Zhu, Y. Li, W. Meng, H. Zhou, et al., A novel mixed potential NH3 sensor based on TiO2@WO3 core–shell composite sensing electrode, Electrochimica Acta, 193(2016) 302-10.
[57] X. Liang, T. Zhong, H. Guan, F. Liu, G. Lu, B. Quan, Ammonia sensor based on NASICON and Cr2O3 electrode, Sensors and Actuators B: Chemical, 136(2009) 479-83.
[58] D. Schönauer, K. Wiesner, M. Fleischer, R. Moos, Selective mixed potential ammonia exhaust gas sensor, Sensors and Actuators B: Chemical, 140(2009) 585-90.
[59] X.D. Li, Y. Chen, L.H. Zhou, F. Xia, J.Z. Xiao, Mg2CuxFe1O3. 5+ x Mixed Metal Oxides as Ammonia Sensitive Material of Ammonia Sensors, Key Engineering Materials, Trans Tech Publ2014, pp. 851-7.
[60] X. Li, C. Wang, B. Wang, Y. Yuan, J. Huang, H. Zhang, et al., Effects of sintering temperature on the NH3 sensing properties of Mg2Cu0.25Fe1O3.75 electrode for YSZ-based potentiometric NH3 sensor, Ceramics International, (2015).
[61] I. Gul, W. Ahmed, A. Maqsood, Electrical and magnetic characterization of nanocrystalline Ni–Zn ferrite synthesis by co-precipitation route, Journal of Magnetism and Magnetic Materials, 320(2008) 270-5.

[62] K. Maaz, S. Karim, A. Mumtaz, S. Hasanain, J. Liu, J. Duan, Synthesis and magnetic characterization of nickel ferrite nanoparticles prepared by co-precipitation route, Journal of Magnetism and Magnetic Materials, 321(2009) 1838-42.
[63] Z. Zi, Y. Sun, X. Zhu, Z. Yang, J. Dai, W. Song, Synthesis and magnetic properties of CoFe2O4 ferrite nanoparticles, Journal of Magnetism and Magnetic Materials, 321(2009) 1251-5.
[64] Y. Xiao, X. Li, J. Zai, K. Wang, Y. Gong, B. Li, et al., CoFe 2 O 4-graphene nanocomposites synthesized through an ultrasonic method with enhanced performances as anode materials for Li-ion batteries, Nano-Micro Letters, 6(2014) 307-15.
[65] C. Peng, B. Chen, Y. Qin, S. Yang, C. Li, Y. Zuo, et al., Facile ultrasonic synthesis of CoO quantum dot/graphene nanosheet composites with high lithium storage capacity, ACS nano, 6(2012) 1074-81.